Implied risk neutral densities from option prices: hypergeometric, spline, lognormal and edgeworth functions

Andre Santos and João Guerra

UNIVERSIDADE TÉCNICA DE LISBOA

Abstract

This work examines the stability and accuracy of four different methods to estimate Risk-Neutral Density functions (RNDs) using European options. These methods are the Double-Lognormal Function (DLN), the Smoothed Implied Volatility Smile (SML), the Density Functional Based on Confluent Hypergeometric function (DFCH) and the Edgeworth expansions (EE).

These methodologies were used to obtain the RNDs from the option prices with the underlying USDBRL (price of US dollars in terms of Brazilian reals) for different maturities (1, 3 and 6 months), and then tested in order to analyze which method best fits a simulated "true" world as estimated through the Heston model (accuracy measure) and which model has a better performance in terms of stability.

We observed that in the majority of the cases the DFCH and DLN outperformed the SML and the EE methods in capturing the "true" implied skewness and kurtosis. However, due to the higher sensitivity of the skewness and kurtosis measures to the tails of the distribution (all the information outside the available strike prices is extrapolated and the probability masses outside this range can have infinite forms) we also compared the tested models using the root mean integrated squared error (RMISE) which is less sensitive to the tails of the distribution. We observed that using the RMISE criteria, the DFCH outperformed the other methods as a better estimator of the "true" RND.

Key words: Risk–neutral density; Option pricing, Natural spline, Hypergeometric function, Double-Lognormal, Edgeworth function, Heston model

1 Introduction

It is accepted by market participants that the prices of financial derivatives provide information about future expectations of the underlying asset prices, especially forwards, futures and options. Forwards and futures only give us the expected value for the underlying asset under the assumptions of risk

neutrality, which makes using cross-sections of observed option prices more attractive because they allow estimation of an implied probability density function.

It is known that the Black and Scholes model has several limitations, because it assumes that the price of the underlying asset evolves according to the geometric Brownian Motion (GBM) with a constant expected return and a constant volatility. The volatility is constant until maturity and also across all quoted strikes, which ignores phenomena like volatility smile and as such distorts probabilities for extreme scenarios. In fact, higher volatilities for strike prices deep out-of-the-money make it more likely that future prices will be very different from current market values. This in turn increases the probability of these option prices being in-the-money in the future and leads to more expensive prices for deep out-of-the-money options, when compared to prices calculated through the B&S model. This results in fatter tails of the true probability density function (pdf) when compared with a lognormal pdf.

To tackle these problems, various methods have been suggested to extract Risk-Neutral Density Functions (RNDs) from option prices and several studies have been carried out to examine the robustness of these estimates and their information power.

In this work we compare four methods of extracting RNDs from USD-BRL European type exchange rate options. These methods are the Double-Lognormal Function, the Smoothed Implied Volatility Smile, the Density Functional Based on Confluent Hypergeometric function and the Edgeworth expansions. We test the stability of the estimated RNDs and their robustness as regards small errors by randomly perturbing option prices by half of the quotation of the tick size as in Bliss and Panigirtzoglou (2002) before re-estimating the RNDs and their accuracy by experimenting their capacity to recover the "true" RNDs. The "true" probability density function (pdf) was estimated using the method developed in Cooper (1999), who generated pseudo prices from Heston's stochastic volatility model, and then compared the performance of the different methods using Monte Carlo simulations in order to obtain RNDs, whereby the input was the option prices calculated by these pseudo prices.

The remainder of this work is organized into seven chapters. Chapter Two gives a presentation of the Black and Scholes model and its theoretical background. In this chapter, we also describe how option prices can provide information about implied probabilities given by market participants to future events and its use as an instrument to extract probability density functions of future prices using the formula proposed in Breeden and Litzenberger (1978).

Chapter Three describes the five models used in this work (DLN, SML, DFCH, EE and Heston). Jondeau et al. (2006) divide the alternative methods into two categories: structural and non-structural. A structural model assumes a specific dynamic for the price or volatility process. A non-structural method allows the estimation of a RND without describing any evolving process for the price or volatility of the underlying asset. The non-structural approaches can be divided into three subcategories: parametric (propose a form for the

RND without assuming any price dynamics for the underlying asset), semi-parametric (suggest an approximation of the true RND) and non-parametric models (do not propose an explicit form for the RND).

Chapter Four describes the measures used to evaluate the performance of the four models tested (MLN, SML, DFCH and EE) in terms of accuracy and stability.

The results of the Monte Carlo simulation experiments and the comparisons of the models tested are presented and discussed in Chapter Five and Six. In Chapter Five we analyze the accuracy and stability performance using the "true" RNDs generated by the Heston parameters proposed in Cooper (1999). In Chapter Six, a similar analysis was carried out. However, the "true" RNDs were obtained through the previously calibrated Heston parameters. The Heston parameters were calibrated taking into account the observed quotes for the USDBRL European options between June 2006 and February 2010.

The historical RND summary statistics obtained using the DLN, SML, DFCH and EE methods for the USDBRL in the time period described above are presented in Chapter Seven.

Finally, Chapter Eight presents the conclusions.

2 Standard option pricing and extraction of RND

2.1 Black & Scholes model

The widely used Black and Scholes model Black and Scholes (1973) for option pricing assumes that the underlying asset price has a lognormal distribution and evolves until reaching maturity in line with a geometric Brownian motion (GBM) stochastic process, with a constant expected return and a constant volatility:

$$dS_t = S_t \mu dt + S_t \sigma dW_t \tag{1}$$

where S_t is the price of the underlying asset at time t, dS_t denotes instantaneous price change, μ is the expected return, σ is the standard deviation of the price process and dW are increments from a Brownian motion process. The parameters μ and σ are assumed to be constant. Besides constant volatility during the term of the option, the B&S model also assumes the same volatility across the whole range of strike prices.

The Black and Scholes Pricing formulas for european call and put options are:

$$C(S;t) = SN(d_1)\text{-}Xe^{-r(T-t)}N(d_2) \; ; \; S > 0 \; ; \; t \in [0;T] \tag{2}$$

$$P(S;t) = Xe^{-r(T-t)}N(-d_2) - SN(-d_1) \; ; \; S > 0 \; ; \; t \in [0;T] \tag{3}$$

with

$$d_1 = \frac{\ln(\frac{S}{X}) + (r + \frac{1}{2}\sigma^2)(T-t)}{\sigma\sqrt{(T-t)}} \tag{4}$$

and

$$d_2 = \frac{\ln(\frac{S}{X}) + (r - \frac{1}{2}\sigma^2)(T-t)}{\sigma\sqrt{(T-t)}} \tag{5}$$

In a world in which prices are lognormally distributed with constant volatility and expected returns it is possible to create a risk free portfolio using delta hedging. The return of this hedged portfolio becomes certain and does not depend on the change of the stock price.

2.2 Relation between option prices and the extraction of RNDs

It is possible to combine call options that have the same time to maturity but different exercise prices, in order to obtain a payoff at expiration that is dependent on the state of the economy at a particular time. The price of these combined securities (state-contingent securities) also reflects the probabilities that investors attribute to those particular states in the future.

This relation between probabilities and the price of a contingent claim [1] was initially proposed in Arrow (1964) who applied a contingent claim model to the securities market. It was shown that the prices of an elementary claim (Arrow-Debreu security) [2] are proportional to the risk-neutral probabilities attached to each of the states.

This Arrow-Debreu security has an important information value and can be replicated with a combination of European call options, called *butterfly spread*, which consists of a long position in two calls with strikes $(X - \Delta M)$ and $(X + \Delta M)$ and a short position in two calls with strike (X) , where $\Delta M > 0$.

Breeden and Litzenberger (1978) applied the developments by Arrow and Debreu and used a state contingent claim in the form of a *butterfly spread* to show that the second partial derivative of a call option pricing function with respect to the strike prices yields the discounted RND $(f(S_T) \times e^{-rT})$.

These authors showed that a portfolio which contains $(1/\Delta^2)$ units of a butterfly spread is determined by the second partial derivative of the European call option with respect to the exercise price:

$$\frac{[c(M-\Delta,T) - c(M,T)] - [c(M,T) - c(M+\Delta,T)]}{\Delta M^2} \tag{6}$$

The payoff of this portfolio at maturity is $\left\{\begin{matrix} dK+|S_T-K| \text{ if } S_T \in [K-dK, K+dK] \\ 0 \text{ elsewhere} \end{matrix}\right\}$. The area under the payoff function is one. Applying this relation to a range of

[1] a claim that can be made when a specific outcome occurs.

[2] a security paying one unit if a state s occurs and zero otherwise.

continuum possible values for the underlying asset, leads to the estimation of the discounted Risk-Neutral Density.

$$\frac{d^2C(X,T)}{dX^2} = e^{-rT} f(S_T) \tag{7}$$

This condition only holds if $C(X,T)$ is monotonic decreasing and convex in the exercise price, otherwise there are arbitrage opportunities and the RND could be negative [Bahra (1997)].

3 RND estimation - Alternative methods

Despite being widely used, the B&S model has several limitations because the log normal assumption does not hold in practice and calculates prices that are different from market values, which creates the need to analyze and study different methods in order to find a model that is more efficient at capturing market expectations and prices.

In this chapter we give an overview of the methods developed in this work in order to obtain estimates which closely reflect the expectations of the option market.

The optimizations we have performed for the calculus of the theoretical option prices and estimation of the risk-neutral densities using the tested models were produced using the MATLAB software. The numerical aspects of the optimizations and the matlab algorithms are shown in Santos (A. D.).

3.1 Structural Models

3.1.1 RND estimation using a model based on stochastic volatility - Heston Model

The Heston Model was developed in Heston (1993) and represents the classical stochastic volatility pricing model. It is used in this work to estimate the density corresponding to the 'true' world. This method adds a second Wiener Process to the price dynamics (volatility modeling), which leads to the dynamics of the underlying asset price (S_t) based on the geometric Brownian Motion with time varying volatility

$$\begin{aligned} dS_t &= \mu S_t dt + S_t \sqrt{v_t} dZ_{1,t} \\ dv_t &= \kappa(\theta - v_t)dt + \sigma_v \sqrt{v_t} dZ_{2,t} \end{aligned} \tag{8}$$

where $\sqrt{v_t}$ denotes current volatility of the underlying asset price, $Z_{1,t}$ and $Z_{2,t}$ represents the correlated Brownian motion processes with correlation parameter ρ, v_t is the volatility of the underlying asset, θ is the long run volatility, σ_v is the volatility of the volatility process and κ is the speed at which the volatility returns to its long run average.

These parameters guide the trajectory of the square root process, which means that along its path, v_t goes around θ, crossing the long run volatility more frequently when k is higher and the trajectory of v_t is more volatile when σ is higher.

The parameter ρ defines the correlation between returns and volatility and can change the form of the RND, generating skewness in asset returns. For example, if $\rho > 0$ the volatility of the asset price increases when the asset price increases, and in this way the weight of the right tail of RND will increase. In contrast, when $\rho < 0$ the decrease in price leads to an increase in volatility and the weight of the left tail of RND will increase.

Heston introduced the following closed formula for the European call option price:

$$
\begin{aligned}
C(S_t, v_t, X, T) &= S_t e^{-r^*(T-t)} P_1 - X e^{-r(T-t)} P_2 \ ; \ S > 0 \ ; \ t \in [0; T], \quad (9)\\
P_j &= \frac{1}{2} + \frac{1}{\pi} \int_0^\infty \mathrm{Re}[\frac{e^{-i\phi \ln(k)} f_j(\ln(S_t), v_0, T-t, \phi)}{i\phi}] d\phi,\\
f_j(\ln(S_t), v_0, T-t, \phi) &= e^{C(T-t,\phi) + D(T-t,\phi) v_t + i\phi \ln(S_t)},\\
C(T-t, \phi) &= (r - r^*)\phi i (T-t) + \frac{a}{\sigma_v^2}\{(b_j - \rho\sigma_v \phi i + d)(T-t)\\
&\quad - 2\ln[\frac{1 - g e^{d(T-t)}}{1-g}]\},\\
D(T-t, \phi) &= \frac{b_j - \rho\sigma_v\phi i + d}{\sigma_v^2}[\frac{1 - e^{d(T-t)}}{1 - g e^{d(T-t)}}],\\
g &= \frac{b_j - \rho\sigma_v \phi i + d}{b_j - \rho\sigma_v \phi i - d},\\
d &= \sqrt{(\rho\sigma_v \phi i - b_j)^2 - \sigma_v^2 (2u_j \phi i - \phi^2)},\\
u_1 &= \frac{1}{2}, u_2 = -\frac{1}{2}, a = \kappa\theta, b_1 = \kappa + \lambda - \rho\sigma_v, b_2 = \kappa + \lambda, i = \sqrt{-1}
\end{aligned}
$$

3.2 Non-Structural Models

3.2.1 Parametric models

3.2.1.1 Mixture of lognormal distribution The mixture of lognormals (MLN) was proposed by Bahra (1997) and Melick and Thomas (1997) and assumes a functional form for the risk-neutral density (RND) that accomodates various stochastic processes for the underlying asset price. Instead of specifying a dynamic for the underlying asset price (which leads to a unique terminal value), it is possible to make assumptions about the functional form of the RND function itself and then obtain the parameters of the distribution by minimizing the distance between the observed option prices and those that are generated by the assumed parametric form. According to the authors, this makes this model more flexible than the Black and Scholes model and increases its ability to capture the main contributions to the smile curve, namely the skewness and the kurtosis of the underlying distribution.

It is known that the prices of European call and put options can be expressed as the discounted sum of all expected future payoffs:

$$C_0(X,T) = e^{-rT}\int_X^\infty q(S_t)(S_t - X)dS_t \tag{10}$$
$$P_0(X,T) = e^{-rT}\int_X^\infty q(S_t)(X - S_t)dS_t$$

According to Bahra (1997), any functional form for the RND $q(S_t)$ can be assumed because the parameters would be estimated through optimization (minimizing the difference between the prices obtained through the MLN model and market prices). Nevertheless, the author assumed that the asset price distributions are closer to the lognormal distribution and consequently it would be plausible to use a weighted sum of lognormal density functions,

$$q(S_t,\theta) = \sum_{i=1}^{k}[w_i L(\alpha_i,\beta_i,S_t)] \tag{11}$$

where $L(\alpha_i,\beta_i,S_t)$ is the ith lognormal distribution with parameters α_i and β_i . It has the following expression:

$$L(\alpha_i,\beta_i,S_t) = \frac{1}{S_t\beta_i\sqrt{2\pi}}e^{[-(\ln(S_t)-\alpha_i)^2/2\beta_i^2]}, \tag{12}$$
$$\alpha_i = \ln(S_t) + (\mu_i - \frac{1}{2}\sigma_i^2)(T-t),$$
$$\beta_i = \sigma_i\sqrt{(T-t)}.$$

The term θ represents the vector of unknown parameters α_i, μ_i, σ_i for $i = 1,...,k$, and k defines the number of mixtures describing the RND. In order to guarantee that q is a probability density, $w_i \geqslant 0$ for $i = 1,...k$, and $\sum_{i=1}^{k} w_i = 1$. In this way q will be a combination of the lognormal densities.

While Melick and Thomas applied this method on the extraction of RNDs from the prices of American options on crude oil futures using a mixture of three independent lognormals, Bahra obtained the RNDs using European options on LIFFE equity index, LIFFE interest rate options and Philadelphia Stock Exchange currency options using a mixture of two independent lognormals. The choice of a mixture of two lognormals is based on the lower number of parameters to be estimated (5 parameters). In fact, options are traded across a relatively small range of exercise prices, hence there are limits on the number of parameters that can be estimated from the data.

Extending the mixture of lognormals to the European call option prices given by equation (10) we have the following option prices for each strike

price (X_i) and with time to maturity $\tau = (T - t)$:

$$c(X_i, \tau) = e^{-r\tau} \int_X^\infty (S_t - X) \sum_{i=1}^k w_i L(\alpha_i, \beta_i, S_T) dS_t, \tag{13}$$
$$c(X_i, \tau) = e^{-r\tau} \sum_{i=1}^k w_i \int_X^\infty (S_t - X) L(\alpha_i, \beta_i, S_T) dS_t.$$

The integral in equation (13) can be rewritten as (see Jondeau et al. (2006)):

$$\begin{aligned} c(X_i, \tau) = & e^{-r\tau} \sum_{i=1}^k w_i e^{\alpha_i + \frac{1}{2}\beta_i^2} N\left(\frac{-\ln(X) + \alpha_i + \beta_i^2}{\beta_i}\right) \\ & - e^{-r\tau} X \sum_{i=1}^k N\left(\frac{-\ln(X) - \alpha_i}{\beta_i}\right]. \end{aligned} \tag{14}$$

Applying the mixture of two lognormals used by Bahra, we get the following closed formula for a European call option,

$$\begin{aligned} c(X, \tau) = & e^{-r\tau} \{ w[e^{\alpha_1 + \frac{1}{2}\beta_1^2} N(d_1) - X N(d_2)] \\ & + (1 - w)[e^{\alpha_2 + \frac{1}{2}\beta_2^2} N(d_3) - X N(d_4)] \} \end{aligned} \tag{15}$$

where

$$\begin{aligned} d_1 &= \frac{-\ln(X) + \alpha_1 + \beta_1^2}{\beta_1}, \\ d_2 &= d_1 - \beta_1, \\ d3 &= \frac{-\ln(X) + \alpha_2 + \beta_2^2}{\beta_2}, \\ d_4 &= d_3 - \beta_2. \end{aligned} \tag{16}$$

For the European put option, Bahra presented the following pricing formula,

$$\begin{aligned} p(X, \tau) = & e^{-r\tau} \{ w[-e^{\alpha_1 + \frac{1}{2}\beta_1^2} N(-d_1) - X N(-d_2)] \\ & + (1 - w)[-e^{\alpha_2 + \frac{1}{2}\beta_2^2} N(-d_3) - X N(-d_4)] \}. \end{aligned} \tag{17}$$

In order to find the parameters of the implied RND (vector θ) we have to solve the minimization problem,

$$\begin{aligned} & \min_{\alpha_1, \alpha_2, \beta_1, \beta_2, w_i} \sum_{i=1}^n [c(X, \tau) - \widehat{c}]^2 + \sum_{i=1}^n [p(X, \tau) - \widehat{p}]^2 \\ & + [w e^{\alpha_1 + \frac{1}{2}\beta_1^2} + (1 - w) e^{\alpha_2 + \frac{1}{2}\beta_2^2} - e^{r\tau} S] \end{aligned} \tag{18}$$

where the first two terms refer to the sum of the squared deviation between option prices estimated through MLN and the observed market prices. Call and put prices can be considered in equation (18) because both refer to the

same underlying distribution. The third term of the equation states that the expected value of the RND must be equal to the forward price of the underlying asset in order to avoid the violation of the arbitrage condition (martingale condition). After estimating parameters $\alpha_1, \alpha_2, \beta_1, \beta_2, w$, we insert them into equation (11) and then the implied RND is obtained.

The optimization problem (18) can be affected by a problem related to the symmetry between the densities because in an optimization program, various parameter vectors can be associated to the same density, which in turn can result in numerically unstable programs where the optimizer goes round in an infinite loop. In Jondeau et al. (2006), the authors recommended the imposition of $\beta_1 > \beta_2$ (first density will have a larger standard deviation than the second one) in order to avoid this symmetry problem.

3.2.1.2 Mixture of hypergeometric functions This method allows the estimation of a probability density function (pdf) without assuming a specific functional form for it. It consists of the use of a formula that encompasses various densities, such as normal, gamma, inverse gamma, weibull, pareto and mixtures of these probability densities.

In Abadir and Rockinger (2003), the authors developed a function based on the confluent hypergeometric function (${}_1F_1$), also known as the function for the case of double integrals of densities. These authors believe the usefulness of ${}_1F_1$ relies on the fact that it includes special cases of incomplete gamma, normal distributions and mixtures of the two. In fact, this function has the advantage of being more efficient than fully nonparametric estimation for small samples and more flexible than parametric methods because it does not restrict functional forms.

The Kummer function ${}_1F_1$ can be defined by:

$$
\begin{aligned}
{}_1F_1 &\equiv \sum_{j=0}^{\infty} \frac{(\alpha)_j}{\beta_j} \frac{z^j}{j!} \equiv 1 + \frac{\alpha}{\beta} z + \frac{\alpha(\alpha+1)}{\beta(\beta+1)} \frac{z^2}{2} + \frac{\alpha(\alpha+1)}{\beta(\beta+1)} \frac{z^2}{2} + ..., \qquad (19) \\
(\alpha)_j &\equiv (\alpha)(\alpha+1)...(\alpha+j-1) \equiv \frac{\Gamma(a+j)}{\Gamma(a)}
\end{aligned}
$$

with $\Gamma(v)$, for $v \in \mathbb{R}$ being the gamma function and $\beta \in \mathbb{N}$.

The function considered for option pricing is called DFCH (density function based on confluent hypergeometric functions) and specifies the European call price as a mixture of two confluent hypergeometric functions:

$$
\begin{aligned}
C(X) = c_1 + c_2 X + l_{X>m_1} a_1((X-m_1)^{b_1}) {}_1F_1(a_2; a_3; b_2(X-m_1)^{b_3}) \qquad (20) \\
+ (a_4) {}_1F_1(a_5; a_6; b_4(X-m_2)^2),
\end{aligned}
$$

where $a_{3,}a_6 \in \mathbb{N}$, $b_2, b_4 \in \mathbb{R}^-$ and $a_{,}, a_2, a_4, a_5, b_1, b_3 \in \mathbb{R}$. The indicator function l represents a component of the density with bounded support.

The first ${}_1F_1$ function can represent a gamma or other asymmetric generalizations, whereas the second ${}_1F_1$ covers symmetric quadratic exponentials,

such as the normal.

To get the implied probability density function, the formula stated in equation (7) is applied to $C(X)$:

$$e^{-rT}f(X) = \frac{d^2C(X)}{dX^2} = l_{X>m1}a_1(X-m_1)^{b1-2}[b_1(b_1-1)_1F_1(a_2;a_3;b_2(X-m_1)^{b_3}) \tag{21}$$

$$\begin{aligned}
&+ \frac{a_2}{a_3}b_2b_3(2b_1+b_3-1)(X-m_1)^{b_3} \\
&\times_1 F_1(a_2+1;a_3+1;b_2(X-m_1)^{b_3}) + \frac{a_2(a_2+1)}{a_3(a_3+1)}b_2^2b_3^2(X-m_1)^{2b_3} \\
&\times_1 F_1(a_2+2;a_3+2;b_2(X-m_1)^{b_3})] \\
&+ 2a_4\frac{a_5}{a_6}b_4[{}_1F_1(a_5+1;a_6+1;b_4(X-m_2)^2) \\
&+ 2\frac{a_5+1}{a_6+1}b_4(X-m_2)^2{}_1F_1(a_5+2;a_6+2;b_4(X-m_2)^2)].
\end{aligned}$$

The integral of the density is given by:

$$\begin{aligned}
\frac{dC(X)}{dX} &= c_2 + l_{X>m_1}a_1(X-m_1)^{b_1-1}[(b_1)_1F_1(a_2;a_3;b_2(X-m_1)^{b_3}) \\
&+ \frac{a_2}{a_3}b_2b_3((X-m_1)^{b_3})_1F_1(a_2+1;a_3+1;b_2(X-m_1)^{b_3})] \\
&+ 2a_4\frac{a_5}{a_6}b_4(X-m_2)_1F_1(a_5+1;a_6+1;b_4(X-m_2)^2).
\end{aligned} \tag{22}$$

As stated above, some restrictions must be set in order to guarantee that $f(X)$ integrates to 1 between X_l and X_u,

$$\int_{X_l}^{X_u} f(X)dX = 1. \tag{23}$$

Through these restrictions, we obtained the following expressions for c_2 and a_4 (the details are presented in the Appendix).

$$\begin{aligned}
c_2 &= -1 + a_4\sqrt{-b_4\pi}, \\
a_4 &= \frac{1}{2\sqrt{-b_4\pi}}\left[1 - a_1(-b_2)^{-a_2}\frac{\Gamma(a_3)}{\Gamma(a_3-a_2)}\right].
\end{aligned} \tag{24}$$

As X tends to ∞, the value of the call option price will be approximately 0 ($C(\infty) = 0$), which is the obvious conclusion for call options very nearly out of the money (the probability to become in the money is near 0). The option value in equation (20) will pay a minimum of c_1, which leads to the following simplification:

$$c_1 = -c_2m_2$$

Using assumptions $b_1 = 1 + a_2 b_3, a_5 = -\frac{1}{2}, a_6 = \frac{1}{2}$, formula (20) can be further simplified (see Abadir and Rockinger (2003)).

The final reduction was based on the no-arbitrage condition $S_t = \exp^{-r(T-t)} E(S_T)$, with r being the risk free rate and $E(X)$ the expected value of the underlying price at maturity,

$$E(X) = a_1 \frac{\Gamma(a_3)}{\Gamma(a_3 - a_2)} (-b_2)^{-a_2} (m_1 - m_2) + m_2. \tag{25}$$

With the restrictions defined above, the number of parameters to estimate in the calculation of the theoretical price in equation (20) is reduced to seven.

In order to obtain the implicit RND we have to proceed with the following minimization problem:

$$\min_{a_2, \alpha_3, b_2, b_3, b_4, m_1, m_2} \sum_{i=1}^{n} [c(X_i, \tau) - \widehat{c}_i]^2 \tag{26}$$

where a_2, a_3, b_2, b_3, b_4, m_1 and m_2 are the parameters to be estimated. Given the restrictions above, $c(X, \tau)$ is the theoretical price given in equation (20), $\widehat{c}$ are the option prices observed in the market and n is the number of strike prices. The RND is obtained by inserting the parameters into equation (21).

3.2.2 Semi-parametric models

3.2.2.1 Edgeworth expansions The Black and Scholes assumption of a lognormal distribution for the underlying asset is relaxed by this method that uses a more flexible distributional form of an Edgeworth series expansion around a lognormal distribution. This technique was developed by Jarrow and Rudd (1982) and captures deviations from log-normality by an Edgeworth expansion. The original Edgeworth expansion use the standard normal as the approximating distribution (see Kendall (1945)). Edgeworth expansions are conceptually similar to Taylor expansions, but are applied to densities instead of points.

To demonstrate how Edgeworth expansion can be obtained lets consider the true cdf F, the aproximating cdf L, the fdp f, the fdp l, its random variable S_T and the characteristic function of F ($\phi_F(u) = \int_{-\infty}^{\infty} e^{ius} f(s) ds$). Given n moments $u_j(F)$ exist, the first $n-1$ cumulants $k_j(F)$ also exist and are defined by the expansion (cumulant-generating function)

$$\log(\phi_F(u)) = \sum_{j=1}^{n-1} k_j(F) \frac{(it)^j}{j!} + o(u^{n-1}). \tag{27}$$

Thus, if the characteristic function $\phi_F(u)$ is known, it is possible to obtain the cumulants by taking an expansion of its logarithm around $u = 0$.

The relationships between moments and cumulants up to fourth order are

$$k_1(F) = u_1(F) = E(S_T), \tag{28}$$
$$k_2(F) = u_2(F) = Var(S_T), \tag{29}$$
$$k_3(F) = u_3(F) = E[(S_T - E[S_T])^3], \tag{30}$$
$$k_4(F) = u_4(F) - 3u_2^2(F) = E[(S_T - E[S_T])4] - 3Var(S_T)^2. \tag{31}$$

The same notation is applied to the approximating cdf L.

Jarrow and Rudd (1982) show that after imposing the equality of the first moment of the approximating density and true density, the implied probability density function can be written as (see appendix):

$$\begin{aligned} f(S_T) = l(S_T) + \frac{k_2(F) - k_2(L)}{2!}\frac{d^2 l(S_T)}{dS_T^2} - \frac{k_3(F) - k_3(L)}{3!}\frac{d^3 l(S_T)}{dS_T^3} \\ + \frac{(k_4(F) - k_4(L)) + 3(k_2(F) - k_2(L))^2}{4!}\frac{d^4 l(S_T)}{dS_T^4} + \varepsilon(S_T), \end{aligned} \tag{32}$$

where $\varepsilon(S_T)$ captures the neglected terms of this fourth order expansion around the true cdf $L(S_T)$, the second term of the expansion denotes differences in variance between $f(S_T)$ and $l(S_T)$ and the third and fourth terms of the expansion adjust $l(S_T)$ to account diferences in skewness and kurtosis respectively. Jarrow and Rudd (1982) suggest that with a good choise for the approximating density, the remainder terms of the expansion $\varepsilon(S_T)$ are likely to be negligible. Because of its use in option pricing theory, Jarrow and Rudd suggested the lognormal distribution $l(S_T)$ as the approximating function. Due to the multicolinearity problem between the second and the fourth moments Jarrow and Rudd (1982) also imposed $k_2(F) = k_2(L)$.

After imposing the equalities of the first and second moments of the approximating and true densities and using the fdp given in equation (32) in equation (10) we have the following option prices for each strike price (X_i) and with time to maturity $\tau = (T - t)$:

$$\begin{aligned} C(F) = C(L) - e^{-rT}\frac{k_3(F) - k_3(L)}{3!}\frac{dl(X)}{dS_T} \\ + e^{-rT}\frac{(k_4(F) - k_4(L)) + 3(k_2(F) - k_2(L))^2}{4!}\frac{d^2 l(K)}{dS_T^2} \end{aligned} \tag{33}$$

Rather than estimating the cumulants $k_3(F)$ and $k_4(F)$, Corrado and Su (1986) rewrote equation (33) in order to estimate directly skewness, $\gamma_1(F)$, and kurtosis, $\gamma_2(F)$, using the relationships:

$$\begin{aligned} \gamma_1(F) &= \frac{k_3(F)}{k_2(L)^{3/2}}, \\ \gamma_2(F) &= \frac{k_4(F)}{k_2(L)^2}, \end{aligned} \tag{34}$$

thus obtaining:

$$C(F) = C(L) - e^{-rT}(\gamma_1(F) - \gamma_1(L))\frac{k_2(L)^{3/2}}{3!}\frac{dl(X)}{dS_T} \tag{35}$$
$$+e^{-rT}(\gamma_2(F) - \gamma_2(L))\frac{k_2(L)^2}{4!}\frac{d^2l(K)}{dS_T^2},$$

where the partial derivatives of the lognormal function are:

$$\frac{dl(S_T)}{dS_T} = -\left(1 + \frac{\log(S_T) - m}{\sigma_\tau^2}\right)\frac{l(S_T)}{S_T}, \tag{36}$$

$$\frac{d^2l(S_T)}{dS_T^2} = -\left(2 + \frac{\log(S_T) - m}{\sigma_\tau^2}\right)\frac{1}{S_T}\frac{dl(S_T)}{dS_T} - \frac{1}{S_T^2\sigma_\tau^2}l(S_T), \tag{37}$$

$$\frac{d^3l(S_T)}{dS_T^3} = -\left(3 + \frac{\log(S_T) - m}{\sigma_\tau^2}\right)\frac{1}{S_T}\frac{d^2l(S_T)}{d^2S_T} - \frac{2}{S_T^2\sigma_\tau^2}\frac{dl(S_T)}{dS_T} + \frac{1}{S_T^3\sigma_\tau^2}l(S_T), \tag{38}$$

$$\frac{d^4l(S_T)}{dS_T^4} = -\left(4 + \frac{\log(S_T) - m}{\sigma_\tau^2}\right)\frac{1}{S_T}\frac{d^3l(S_T)}{d^3S_T} - \frac{3}{S_T^2\sigma_\tau^2}\frac{d^2l(S_T)}{dS_T^2} + \frac{3}{S_T^3\sigma_\tau^2}\frac{dl(S_T)}{dS_T} \tag{39}$$

$$-\frac{2}{S_T^4\sigma_\tau^2}l(S_T), \tag{40}$$

with $m = \log(S_t) + (r - \frac{\sigma^2}{2})$. The parameters to be estimated in equation (35) are the implied volatility, σ^2, skewness, $\gamma_1(F)$, and kurtosis, $\gamma_1(F)$.

3.2.3 Non-parametric models

3.2.3.1 Spline methods This method consists of the derivation of the RND using the results of Breeden and Litzenberger (1978), but with a preliminary process of smoothing the volatility smile. The first approach using this method was made by Shimko (1993), who proposed smoothing the volatility smile via a low order polynomial (using a quadratic polynomial) that fitted the implied volatilities (on the y-axis) and the associated strike prices (on the x-axis),

$$\sigma_i = a_0 + a_1K_i + a_2K_i^2, \text{ for } i = 1, ..., N, \tag{41}$$

with N as the number of observed strike prices. The continuous implied volatility function obtained (on strike prices space) is then inserted back into Black and Scholes formula (2) and the probability density function is obtained through $\frac{dC^2}{dS^2}$. The option currency markets are quoted in terms of implied volatility for a specific delta ($\Delta = \frac{dC}{dS}$), which makes it necessary to convert the deltas into strike prices via the Black and Scholes model.

Malz (1996) applied smoothing of the volatility smile using the delta as the x-axis instead of the strike price. Using delta rather than strike, away-from-the-money groups implied volatilities closer than near-the-money implied volatilities, which gives more weight to the centre of the distribution where the data is more reliable (more frequently traded).

Campa et al. (1997) used the spline method instead of the quadratic polynomial to smooth the smile curve. A natural cubic spline was applied using

the strike prices as the X-axis. This method allows the smoothness of the fitted curve to be controlled and is less restrictive about the shape of the fitted function.

Bliss and Panigirtzoglou (2002) applied a natural cubic spline in the volatility/delta space.

The cubic spline interpolation consists of connecting the adjacent points (Δ_i, σ_i), $(\Delta_{i+1}, \sigma_{i+1})$, using the cubic functions $\hat{\sigma}_i; i = 0, ..., n-1$ in order to piece together a curve with continuous first and second order derivatives.

$$\hat{\sigma}_i = \begin{cases} \hat{\sigma}_0(\Delta) & \text{if } \Delta < \Delta_1 \\ \hat{\sigma}_1(\Delta) & \text{if } \Delta_1 < \Delta < \Delta_2 \\ \vdots & \\ \hat{\sigma}_{n-1}(\Delta) & \text{if } \Delta_{n-1} < \Delta < \Delta_n \\ \hat{\sigma}_n(\Delta) & \text{if } \Delta > \Delta_n \end{cases} \tag{42}$$

where $\hat{\sigma}_i$ is a third order polynomial defined by:

$$\hat{\sigma}_i(\Delta) = d_i + c_i(\Delta - \Delta_i) + b_i(\Delta - \Delta_i)^2 + a_i(\Delta - \Delta_i)^3 \tag{43}$$

with Δ being in the interval $[\Delta_i, \Delta_{i+1}]$. At Δ_i the value of the function is d_i.

The first and second derivatives of equation (43) are:

$$\hat{\sigma}_i'(\Delta) = c_i + 2b_i(\Delta - \Delta_i) + 3a_i(\Delta - \Delta_i)^2, \tag{44}$$
$$\hat{\sigma}_i''(\Delta) = 2b_i + 6a_i(\Delta - \Delta_i), \tag{45}$$

which means that the second-order derivative $(\hat{\sigma}_i'')$ is given as a linear interpolation between knot points.

The condition that the cubic functions $\hat{\sigma}_i$ and $\hat{\sigma}_{i-1}$ must meet at the point (Δ_i, y_i) is expressed as:

$$\hat{\sigma}_{i-1}(\Delta_i) = \hat{\sigma}_i(\Delta_i) = y_i \tag{46}$$
$$y_i = d_i = a_{i-1}(\Delta_i - \Delta_{i-1})^3 + b_{i-1}(\Delta_i - \Delta_{i-1})^2 + c_{i-1}(\Delta_i - \Delta_{i-1}) + d_{i-1}$$

The conditions regarding the continuous nature of the first and second derivatives in the knot points are:

$$\hat{\sigma}_{i-1}'(\Delta_i) = \hat{\sigma}_i'(\Delta_i) \tag{47}$$
$$3a_{i-1}(\Delta_i - \Delta_{i-1})^2 + 2b_{i-1}(\Delta_i - \Delta_{i-1}) + c_{i-1} = c_i$$

$$\hat{\sigma}''_{i-1}(\Delta_i) = \hat{\sigma}''_i(\Delta_i) \tag{48}$$
$$6a_{i-1}(\Delta_i - \Delta_{i-1})^2 + 2b_{i-1}(\Delta_i - \Delta_{i-1}) = 2b_i$$

In a natural smoothing spline the second order derivatives in the extreme knot points are 0, $S''(x_0) = 0$ and $S''(x_n) = 0$ (leading to a spline function that is linear outside the range of available data). This condition can result in negative values when extrapolating outside the extreme points, which can yield a negative fitted fdp in the extrapolated points (in this work we did not have this problem). In a natural spline, the smoothness of the interpolating polynomial is controlled by a smoothness parameter λ, which weights the degree of curvature of the spline function. According to Bliss and Panigirtzoglou (2002), the cubic interpolating spline has the disadvantage of following the same random fluctuations as the data points, which distorts the nature of the underlying function, which explains why they used a cubic smoothing spline.

The natural spline minimizes the following objective function:

$$\min_{\theta}(1-\lambda)\sum_{i=1}^{N} w_j(\sigma_i - \hat{\sigma}_i(\Delta_i,\theta))^2 + \lambda\int_{-\infty}^{\infty}(\sigma''(\Delta;\theta))^2 d\Delta, \tag{49}$$

where N is the number of quoted deltas ($\Delta = \frac{dC}{dS}$), $\hat{\sigma}_i(\Delta_i,\theta)$ is the implied volatility corresponding to the spline parameters represented by vector θ and w_i represents the weight attributed to each observation. The first term measure the goodness of fit and the second term measures the smoothness of the spline. If $\lambda = 0$ the cubic spline has an exact fit to the data (the closeness of the spline to the data is the only concern). If $\lambda = 1$ the interpolating function will be a straight line (smoothness is all that matters).

In the estimation of the RNDs through the SML model we used the method proposed in Bliss and Panigirtzoglou (2002).

The variable regarding the weight parameter w in equation (49) is described by Bliss and Panigirtzoglou as a source of price error. It is known that in the context of the Black and Scholes formula, the only unobservable parameter is volatility (σ), which means that the uncertainty regarding the PDF lies in σ. The greek vega (v) measures the relationship between volatility σ and option price ($v = \frac{dC}{d\sigma}$) and reflects the uncertainty concerning the volatility. The value of v is approximately 0 for far deep-out-the-money options and reaches its maximum for at-the-money options [3]. As in Bliss and Panigirtzoglou (2002) we use this v weighting when fitting the volatility smile because this weighting scheme places more weight on near-the-money options and less weight on away-from-the-money options. However, the authors admitted that it was difficult

[3] The value of out-the-money and in-the-money options relies mainly in the intrinsic value. The part that depends of the time value, (which depends on σ) is smaller.

to choose a good weighting scheme that takes into account all the sources of price error. In this work we tested the SML model using both vega weighting ($w_i = v_i$) and equal weighting ($w_i = 1$) and observed that the performance is similar for both (with a slight improvement for the vega weighting).

We also tested this method using the value λ that minimizes the RMISE (root mean integrated squared error). Nevertheless, because in the real world we don't know the "true" RND, we are unable to get the λ that minimizes RMISE. As such, we also performed the SML technique using a specific value for the smoothing parameter ($\lambda = 0.9$).

In conclusion, we tested this method using different schemes for the weighting parameter ($w_i = v_i$ and $w_i = 1$) and for the smoothness of the spline (λ that minimizes the RMISE and $\lambda = 0.9$). We observed that the performance is very similar for the different schemes (see figures B.3 in Appendix B).

4 Accuracy and Stability analysis of the tested PDF estimation methods

4.1 Data

The RNDs analyzed in this work were extracted from currency OTC options with the underlying USDBRL (price of US dollars in terms of Brazilian reals).

The quotes used as inputs were taken from the daily settlement bid prices in Bloomberg for Offshore USDBRL FX Options [4]. The data collected covers the period from June 2006 (half a year before the problems regarding the subprime crisis started to worsen) to February 2010 (seven months after the Brazilian general election) and comprises the monthly quotes (end of month prices).

The calls and puts used are of the European type and are priced in volatility as a function of delta. The grid of quoted deltas is 0.05, 0.1, 0.15, 0.25, 0.35 and 0.5 deltas. This means that we only considered out-of-the money options (calls and puts) and at-the-money options [5], which confirms the general understanding that out-the-money options tend to be more liquid than in-the-money options. In this work, we estimate the RNDs using 1, 3 and 6 months to maturity options.

[4] Information provided by Bloomberg for the OTC Market. The USDBRL is quoted in volatility in terms of delta according to international conventions (does not use the specific maturity of BM&F calendar and a day count of business days/252 just like other financial instruments traded in BM&F)

[5] The delta value varies from 0 for very out-the-money options to 1 for deeply in-the-money options. At the money options have a delta close to 0.5.

4.2 Testing PDF estimation techniques using Monte Carlo approach

To test the accuracy of the tested methods at capturing the risk-neutral density functions, we have to see how closely they fit the true risk-neutral density. Unfortunately, the true RND is unobservable, so we use the method proposed in Cooper (1999). In the absence of the true RND, Cooper suggested the use of simulated option prices data that correspond to a given risk-neutral density function, and then, using these simulated prices as input, test what methods produce a better performance in recovering the given RND.

In order to test the ability of the estimation methods tested to capture a wide range of possible shapes of the "true" RNDs, we establish a set of six scenarios divided into low and high volatility and which have three levels of skewness (strong negative skewness, weak positive skewness and strong positive skewness) as in Cooper (1999) and Bu and Hadri (2007). The authors chose the long-run volatility based on the levels of implied volatility typically observed within equity markets and for the low volatility scenarios chose the long run volatility typically observed in stock index, currency and interest rate markets.

Table 4-1: Parameters used in Heston model under each scenario

	Strong negative Skew	Weak positive skew	Strong positive skew
	Scenario 1	Scenario 2	Scenario 3
Low volatility	$\kappa = 2, \sqrt{\theta} = 0.1$	$\kappa = 2, \sqrt{\theta} = 0.1$	$\kappa = 2, \sqrt{\theta} = 0.1$
	$\sigma = 0.1, \rho = -0.9$	$\sigma = 0.1, \rho = 0$	$\sigma = 0.1, \rho = 0.9$
	Scenario 4	Scenario 5	Scenario 6
High volatility	$\kappa = 2, \sqrt{\theta} = 0.3$	$\kappa = 2, \sqrt{\theta} = 0.3$	$\kappa = 2, \sqrt{\theta} = 0.3$
	$\sigma = 0.4, \rho = -0.9$	$\sigma = 0.4, \rho = 0$	$\sigma = 0.4, \rho = 0.9$

In generating these scenarios, as input we considered a grid of strike prices which results from the average of historical strike prices between January 1996 and February 2010 (end of month prices) for each delta, in order to obtain the average interval between strike prices for this period. Because the quotes are given in volatility in terms of delta, at each considered date, we converted the deltas into strike prices using the formulas

$$\begin{aligned} X_{call} &= S_t e^{-N^{-1}(\Delta_{call} e^{r_{usd}T})\sigma\sqrt{T} + (r_{brl} - r_{usd} + \sigma^2/2)T} \\ X_{put} &= S_t e^{N^{-1}(-\Delta_{put} e^{r_{usd}T})\sigma\sqrt{T} + (r_{brl} - r_{usd} + \sigma^2/2)T} \end{aligned}, \tag{50}$$

where S_t is the USDBRL exchange rate, r_{brl} is the domestic risk-free interest rate (Brazilian interest rate) and r_{usd} the foreign interest rate (US interest rate) Espen (2007). As with strike prices, in the Heston model we also used

the average and the volatility of the spot USDBRL FX rate for the period starting on June 2006 and finishing on February 2010 for S_0 (USDBRL price at $t = 0$) and v_0 (volatility of the USDBRL price at $t = 0$). The interest rates r_{brl} and r_{usd} are also an average from the money market rates (US Libor and SICOR for Brazil) for the same period and have a maturity of 1, 3 or 6 months, depending on the maturity of the "true" RND. In total, we generate six scenarios for each maturity which results in eighteen different RNDs.

Our goal using this method was to produce risk-neutral densities that incorporate the different shapes and scenarios discussed above in order to test the capacity of the MLN, SML, DFCH and EE methods to recover these RNDs. Doing this does not assume that equation (8) explains the asset price dynamics in the real world.

To test the robustness of the MLN, SML, DFCH and EE models in recovering the "true" RNDs, we first derive the call option prices using equation (9) for each combination of scenario and maturity. We then add a uniformly distributed random noise perturbation in prices of size between minus half and half of the tick size (according to BM&FBOVESPA, the minimum tick size is 0.001) as in Bliss and Panigirtzoglou (2002). Given these shocked option prices, we use the MLN, SML, DFCH and EE methods to estimate the RNDs. This process of first shocking prices and then fitting the RND is repeated 500 times for the eighteen combinations of maturities and scenarios (Monte Carlo Simulation).

In order to approximate the methodology described above to the characteristics of the USDBRL option market, we proceed with the calibration of the Heston model for the end of month USDBRL option quotes between June 2006 and February 2010 (the results are presented in figure B.11 in Appendix B) and we also produced the tests described above for 12 dates (6 low volatility dates and 6 high volatility dates). For the low volatility dates we select the period between October 2006 and March 2007 (before the increased problems regarding the subprime crisis). For the high volatility dates we select the period between September 2008 and February 2009 (peak of the financial crisis). For these periods, we generate the "true" RNDs using the calibration parameters and the strike prices obtained for each tested date.

The different methods are then compared using some statistical measures that will be described below.

4.3 Statistics used in comparison of different techniques

In this work the different methods were compared using different approaches adopted by different authors.

In Cooper (1999) and Bliss and Panigirtzoglou (2002) the mean, standard deviation, skewness and kurtosis of the estimated RNDs were analyzed. However, Bliss and Panigirtzolou focused on stability analysis.

In Cooper the robustness of the MLN and SML methods was studied by comparing the mean of the summary statistics obtained from the Monte Carlo

simulations with the summary statistics of the "true" RNDs. The process of shocking the prices [6] and then fitting the RNDs was repeated 100 times. The author also tested the stability of these models by analyzing the standard deviation of the summary statistics, arguing that the model with the best performance in terms of stability has a lower standard deviation for the different descriptive statistics. He concluded that the SML method performed better than the MLN method in terms of accuracy and stability.

Bliss and Panigirtzolou tested the stability of the MLN and SML methods, but instead of shocking the fitted prices obtained from the Heston model, they introduced a noise in market prices. The authors believed a good estimation method would have better behavior in the convergence results of the processed simulations. These authors did not adopt the methods followed by Cooper, arguing that goodness-of-fit results outside the range of available strike prices (tails of the distribution) can be unreliable, in the sense that there is an infinite variety of probability masses in the tails of the RNDs obtained. In fact, the summary statistics with higher moments like skewness and kurtosis are very sensitive to the tails of the distribution, and the data outside the set examined is heavily dependent on the estimation method used. For example, when the assumed PFD has a double-lognormal functional form, the MLN estimation method may do better than the other methods. We agree with these arguments and hence we give more importance to the RMISE analysis (root mean integrated analysis) as in Bu and Hadri (2007).

Bu and Hadri (2007) tested the accuracy and stability of the DFCH and SML methods using the root mean integrated squared error (RMISE), which has the advantage of being less sensitive to the tails of the distribution. Another advantage of RMISE is that it can be broken down into RISB (root integrate square bias) that measures the accuracy and RIV (root integrated variance) which indicates the stability of the distribution. As in Cooper (1999), Bu and Hadri also compared the performance of the methods in terms of a "true" PDF produced from an assumed Heston stochastic volatility price and using the pseudo-prices generated from the PDFs as input. For each combination of maturity and scenario, the authors carry out 500 simulations and find that in the majority of the cases the DFCH method performs better than the SML method in terms of accuracy (RISB) and stability (RIV).

In this work we tested both accuracy and stability of the DFCH, MLN, SML and EE methods using the RMISE as in Bu and Hadri (2007) and using the mean, standard deviation, skewness and kurtosis summary statistics as in Cooper (1999) and Bliss and Panigirtzoglou (2002). We also carry out 500 simulations for each scenario.

A definition of RMISE is provided below:

i. *RMISE*: the root mean integrated squared error. By considering $\hat{f}(S_t)$ as the estimator of the true RND, then the RMISE is defined as

[6] each price was shocked by a random number uniformly distributed from -1/2 to +1/2 a tick size

$$RMISE(\hat{f}) = \sqrt{E[\int_{-\infty}^{\infty} (\hat{f}(S_t) - f(S_t))^2 dS_t]} \tag{51}$$

representing a measure of the average integral of the squared error over the support of the RND. It is a measure of the quality of the estimator and is not as sensitive to the tails of the distribution as the skewness and kurtosis.

The squared of RMISE can also be broken down into the sum of the squared RISB (root integrated squared bias) and squared RIV (root integrated variance):

$$RMISE^2(\hat{f}) = RISB^2(\hat{f}) + RIV^2(\hat{f}) \tag{52}$$

$$RISB(\hat{f}) = \sqrt{\int_{-\infty}^{\infty} (E[\hat{f}(S_t)] - f(S_t))^2 dS_t]} \tag{53}$$

$$RIV(\hat{f}) = \sqrt{\int_{-\infty}^{\infty} E[(\hat{f}(S_t) - E[\hat{f}(S_t)])^2] dS_t} \tag{54}$$

In line with these approaches, the model with better accuracy would present mean values of summary statistics closer to the "true" RND and lower RISB. The model with more stability would have a lower standard deviation of summary statistics and a lower RIV.

5 Comparison of different methods using the Cooper scenarios

5.1 Analysis using mean, standard deviation, skewness and kurtosis

The graphics with the results from these tests are presented in Appendix B (figures B.1, B.2, B.3, B.4).

5.1.1 Accuracy

	Scenarios	Expected Value	Volatility	Skewness	Kurtosis
1 month	low volatility and negative skewness	MLN	SPLINE	HYPERGEOM	HYPERGEOM
	low volatility	MLN	SPLINE	MLN	SPLINE
	low volatility and positive skewness	EDGE	SPLINE	HYPERGEOM	SPLINE
	high volatility and negative skewness	HYPERGEOM	HYPERGEOM	SPLINE	HYPERGEOM
	high volatility	MLN	HYPERGEOM	MLN	MLN
	high volatility and positive skewness	EDGE	EDGE	MLN	MLN
3 months	low volatility and negative skewness	MLN	SPLINE	HYPERGEOM	HYPERGEOM
	low volatility	MLN	SPLINE	MLN	MLN
	low volatility and positive skewness	MLN	SPLINE	HYPERGEOM	MLN
	high volatility and negative skewness	HYPERGEOM	HYPERGEOM	HYPERGEOM	HYPERGEOM
	high volatility	MLN	MLN	MLN	MLN
	high volatility and positive skewness	SPLINE	EDGE	HYPERGEOM	HYPERGEOM
6 months	low volatility and negative skewness	MLN	HYPERGEOM	EDGE	MLN
	low volatility	EDGE	HYPERGEOM	HYPERGEOM	HYPERGEOM
	low volatility and positive skewness	SPLINE	HYPERGEOM	HYPERGEOM	HYPERGEOM
	high volatility and negative skewness	MLN	EDGE	EDGE	EDGE
	high volatility	MLN	SPLINE	MLN	MLN
	high volatility and positive skewness	MLN	HYPERGEOM	HYPERGEOM	HYPERGEOM

Fig. 1. Best method in terms of accuracy for each combination of scenario and maturity

If we look at the expected value, we see that the MLN method outperforms the other models.

Analyzing the volatility, we observe that in general terms the SML method has a better performance in capturing the volatility of the "true" density. The EE underperforms the other methods. The volatility of all tested RNDs increases in line with longer time to maturity, which confirms the higher uncertainty attached to longer maturities.

Considering all the maturities, the DFCH method has skewness values that have a close fit to the "true" skewness when compared to the other models models. The MLN estimator was less biased than the SML estimator. All the models except the EE were able to capture the different levels of skewness corresponding to each scenario, which demonstrates their ability to incorporate the changes in skewness observed in the real world. In fact, the changes of the implied skewness estimated through the EE method were sistematically bellow the changes captured by the other models.

Regarding the implied kurtosis, it can be seen that the DFCH and MLN methods have a close fit in the majority of the scenarios. The EE method has the worst performance in capturing the true kurtosis and showed once again lower changes between the values obtained for the different scenarios. This is due to EE's difficulties accomodating higher moments beyond a certain range (because it can yield negative densities, there is a limited range of skewness and kurtosis combinations that yield positive densities).

5.1.2 Stability

	Scenarios	Volatility	Skewness	Kurtosis
1 month	low volatility and negative skewness	HYPERGEOM	SPLINE	SPLINE
	low volatility	MLN	SPLINE	SPLINE
	low volatility and positive skewness	EDGE	SPLINE	SPLINE
	high volatility and negative skewness	EDGE	SPLINE	SPLINE
	high volatility	HYPERGEOM	SPLINE	SPLINE
	high volatility and positive skewness	EDGE	EDGE	EDGE
3 months	low volatility and negative skewness	EDGE	HYPERGEOM	SPLINE
	low volatility	EDGE	EDGE	EDGE
	low volatility and positive skewness	EDGE	SPLINE	EDGE
	high volatility and negative skewness	SPLINE	EDGE	EDGE
	high volatility	MLN	SPLINE	SPLINE
	high volatility and positive skewness	EDGE	EDGE	EDGE
6 months	low volatility and negative skewness	EDGE	HYPERGEOM	EDGE
	low volatility	MLN	SPLINE	SPLINE
	low volatility and positive skewness	SPLINE	SPLINE	SPLINE
	high volatility and negative skewness	SPLINE	SPLINE	SPLINE
	high volatility	SPLINE	SPLINE	SPLINE
	high volatility and positive skewness	EDGE	EDGE	EDGE

Fig. 2. The most stable method for each combination of scenario and maturity

The SML method has the highest degree of stability in skewness and kurtosis estimations and the EE model is the most stable in capturing the "true" volatility. It should be mentioned that the stability of the SML method increases when the v weighting scheme is applied (see figure B.3 in Appendix B). The DFCH and MLN methods were the most unstable models in capturing the volatility, skewness and kurtosis estimations.

5.2 Analysis using RMISE

	Scenarios	RISB	RMISE	RIV
1 month	low volatility and negative skewness	HYPERGEOM	HYPERGEOM	SPLINE
	low volatility	MLN	MLN	MLN
	low volatility and positive skewness	MLN	MLN	MLN
	high volatility and negative skewness	HYPERGEOM	HYPERGEOM	EDGE
	high volatility	MLN	MLN	EDGE
	high volatility and positive skewness	HYPERGEOM	HYPERGEOM	SPLINE
3 months	low volatility and negative skewness	HYPERGEOM	HYPERGEOM	SPLINE
	low volatility	MLN	MLN	EDGE
	low volatility and positive skewness	MLN	MLN	EDGE
	high volatility and negative skewness	HYPERGEOM	HYPERGEOM	SPLINE
	high volatility	MLN	MLN	SPLINE
	high volatility and positive skewness	MLN	MLN	EDGE
6 months	low volatility and negative skewness	MLN	MLN	EDGE
	low volatility	MLN	MLN	MLN
	low volatility and positive skewness	MLN	MLN	SPLINE
	high volatility and negative skewness	HYPERGEOM	HYPERGEOM	SPLINE
	high volatility	MLN	MLN	SPLINE
	high volatility and positive skewness	MLN	MLN	EDGE

Fig. 3. Best method according to RMISE criteria

The values obtained for the eighteen combinations of scenarios and maturities are presented in figure B.4 in Appendix B.

Examining the results for the different maturities, we observe that the RNDs estimated with the MLN and DFCH methods perform better than the distrib-

utions obtained with the SML in terms of the overall quality of the RND estimator. In fact, the lower RMISE of the MLN and DFCH methods is observed in the majority of the eighteen combinations of scenarios and maturities (the MLN method has the best RND estimator 10 times and the DFCH method 6 times).The EE underperformed the other methods in almost all the scenarios and maturities.

The DFCH method performs less well in terms of accuracy in the central scenarios (lower skewness) and longer maturities. For the longest maturities, the MLN method has a higher overall quality as an estimator (lower RMISE) and better accuracy.

Analyzing the stability through RIV, we conclude that the EE, the MLN and SML methods have a very similar behavior. The DFCH method underperforms in relation to the other methods in the majority of the cases.

As in the analysis of the summary statistics, we examined the results considering the impact on the SML method of using both the v weighting scheme and the equal weighting scheme and the optimal λ (minimizes RMISE) as the smoothing parameter and $\lambda = 0.9$. In terms of the overall quality of the estimator which is measured by RMISE, we observe again a slightly better performance of the SML method when it applies a v weighting approach and an optimal λ.

5.3 Comparison of our results with other studies

In Cooper (1999), the MLN model was compared with the SML method in terms of accuracy and stability using the summary statistics approach and in Bu and Hadri (2007) the DFCH method was compared with the SML method in line with RMISE criteria. In both studies, the accuracy was measured using the Cooper technique of generating the "true" world through the Heston model and the SML was estimated interpolating across the volatility smile in "delta-space" via a cubic smoothing spline (as in our study). In Cooper, the SML method had a better stability performance and in terms of accuracy neither technique outperformed the other in skewness and kurtosis estimates. In Bu and Hadri (2007) the DFCH had a higher accuracy (lower RISB) and the SML method was more stable in the majority of scenarios (lower RIV).

We added the DFCH and EE methods to Cooper analysis. In our study the MLN and DFCH methods outperformed the SML and EE methods in skewness and kurtosis accuracy and the MLN had the less biased "true" volatility estimation. In terms of stability, we obtained the same results as in Cooper. In fact, the higher moments estimated through the SML method were the most stable.

The MLN and EE methods were added to Bu and Hadri's study. According to the RMISE criterion, the MLN and DFCH were the most accurate models in the majority of scenarios (lower RISB) and there was no clear "winner" in terms of stability performance.

6 Comparison of different methods using USDBRL Heston calibrated parameters

The graphics with the results from these tests are presented in Appendix B (figures B.5, B.6, B.7 and B.8).

6.1 Analysis using mean, standard deviation, skewness and kurtosis

6.1.1 Accuracy

		Low volatility dates				High volatility dates			
	Scenarios	Expected Value	Volatility	Skewness	Kurtosis	Expected Value	Volatility	Skewness	Kurtosis
1 month	high volatility and negative skewness	MLN	SPLINE	MLN	HYPERGEOM	HYPERGEOM	HYPERGEOM	HYPERGEOM	MLN
	high volatility	EDGE	SPLINE	HYPERGEOM	HYPERGEOM	HYPERGEOM	HYPERGEOM	HYPERGEOM	MLN
	high volatility and positive skewness	EDGE	SPLINE	HYPERGEOM	HYPERGEOM	EDGE	SPLINE	HYPERGEOM	HYPERGEOM
	high volatility and negative skewness	EDGE	SPLINE	HYPERGEOM	MLN	EDGE	SPLINE	HYPERGEOM	HYPERGEOM
	high volatility	HYPERGEOM	SPLINE	MLN	HYPERGEOM	EDGE	SPLINE	HYPERGEOM	MLN
	high volatility and positive skewness	MLN	EDGE	MLN	HYPERGEOM	HYPERGEOM	HYPERGEOM	HYPERGEOM	HYPERGEOM
3 months	high volatility and negative skewness	EDGE	HYPERGEOM	HYPERGEOM	MLN	EDGE	SPLINE	MLN	HYPERGEOM
	high volatility	EDGE	SPLINE	MLN	HYPERGEOM	EDGE	HYPERGEOM	HYPERGEOM	HYPERGEOM
	high volatility and positive skewness	MLN	HYPERGEOM	MLN	HYPERGEOM	EDGE	HYPERGEOM	HYPERGEOM	MLN
	high volatility and negative skewness	EDGE	SPLINE	HYPERGEOM	MLN	EDGE	HYPERGEOM	HYPERGEOM	HYPERGEOM
	high volatility	MLN	SPLINE	MLN	MLN	HYPERGEOM	HYPERGEOM	HYPERGEOM	HYPERGEOM
	high volatility and positive skewness	EDGE	SPLINE	HYPERGEOM	MLN	HYPERGEOM	HYPERGEOM	HYPERGEOM	HYPERGEOM
6 months	high volatility and negative skewness	EDGE	SPLINE	HYPERGEOM	MLN	SPLINE	MLN	MLN	MLN
	high volatility	EDGE	SPLINE	MLN	MLN	SPLINE	SPLINE	HYPERGEOM	HYPERGEOM
	high volatility and positive skewness	MLN	SPLINE	MLN	HYPERGEOM	SPLINE	SPLINE	HYPERGEOM	MLN
	high volatility and negative skewness	EDGE	SPLINE	MLN	MLN	SPLINE	SPLINE	MLN	MLN
	high volatility	EDGE	SPLINE	MLN	MLN	SPLINE	MLN	HYPERGEOM	HYPERGEOM
	high volatility and positive skewness	EDGE	SPLINE	HYPERGEOM	MLN	SPLINE	MLN	HYPERGEOM	HYPERGEOM

Fig. 4. Best method in terms of accuracy for the low and high volatility dates

6.1.1.1 Low volatility Dates The implied volatility estimated using the SML method has the closest fit to the "true" standard deviation for the majority of dates and maturities. The MLN method performs worse than the SML and DFCH models in capturing the "true" volatility.

The MLN and DFCH methods outperformed the other models in capturing the "true" implied skewness with the MLN being slightly better than the DFCH method.

The implied kurtosis estimated using the MLN method was closer to the "true" kurtosis for most dates and maturities. The DFCH method was better in capturing the "true" kurtosis for 1-month term.

As in Cooper scenarios the EE method was unable to capture the highest moments of the the "true" RNDs and has the worst performance across all the scenarios.

6.1.1.2 High volatility Dates For the high volatility dates, the best volatility fit was estimated using the DFCH method. Apart from EE method, the MLN method has the worst performance in estimating the implied volatility.

The best fit for skewness and kurtosis was estimated using the DFCH method and the MLN outperformed the SML model in capturing the "true" implied kurtosis in the 3 and 6-month terms.

Once again, the EE method has the worst performance in capturing the moments of the "true" densities.

6.1.2 *Stability*

		Low volatility dates			High volatility dates		
	Scenarios	Volatility	Skewness	Kurtosis	Volatility	Skewness	Kurtosis
1 month	low volatility and negative skewness	EDGE	EDGE	EDGE	EDGE	EDGE	EDGE
	low volatility	EDGE	EDGE	EDGE	HYPERGEOM	SPLINE	SPLINE
	low volatility and positive skewness	EDGE	EDGE	EDGE	EDGE	EDGE	EDGE
	high volatility and negative skewness	HYPERGEOM	EDGE	EDGE	MLN	SPLINE	SPLINE
	high volatility	EDGE	SPLINE	EDGE	EDGE	SPLINE	EDGE
	high volatility and positive skewness	MLN	SPLINE	EDGE	SPLINE	SPLINE	SPLINE
3 months	low volatility and negative skewness	EDGE	EDGE	EDGE	EDGE	SPLINE	SPLINE
	low volatility	MLN	SPLINE	EDGE	EDGE	EDGE	EDGE
	low volatility and positive skewness	EDGE	EDGE	EDGE	HYPERGEOM	SPLINE	EDGE
	high volatility and negative skewness	EDGE	EDGE	EDGE	HYPERGEOM	SPLINE	SPLINE
	high volatility	EDGE	EDGE	EDGE	EDGE	SPLINE	SPLINE
	high volatility and positive skewness	HYPERGEOM	EDGE	EDGE	HYPERGEOM	SPLINE	SPLINE
6 months	low volatility and negative skewness	HYPERGEOM	SPLINE	SPLINE	HYPERGEOM	SPLINE	SPLINE
	low volatility	EDGE	SPLINE	EDGE	HYPERGEOM	SPLINE	EDGE
	low volatility and positive skewness	HYPERGEOM	SPLINE	EDGE	EDGE	SPLINE	SPLINE
	high volatility and negative skewness	HYPERGEOM	SPLINE	SPLINE	EDGE	EDGE	EDGE
	high volatility	HYPERGEOM	SPLINE	SPLINE	EDGE	EDGE	EDGE
	high volatility and positive skewness	EDGE	EDGE	EDGE	HYPERGEOM	EDGE	EDGE

Fig. 5. The most stable method for the low and high volatility dates

Regarding the implied volatility estimators, the EE method was the most stable model for the low volatility dates and high volatility dates. The DFCH method outperformed the SML and MLN models.

The EE method was the most stable model in capturing the implied skewness in the low volatility dates and the the SML method outperformed the other models in the high volatility dates. The MLN method was the most unstable model for the majority of the low volatility dates and the DFCH was the least stable model for most of the high volatility dates.

The implied kurtosis estimated through EE method were the most stable for a bigger proportion of the low volatility and high volatility dates. The MLN and DFCH methods performs the worst in terms of stability.

6.2 *Analysis using RMISE*

		Low volatility dates			High volatility dates		
	Scenarios	RMISE	RISB	RIV	RMISE	RISB	RIV
1 month	low volatility and negative skewness	HYPERGEOM	HYPERGEOM	EDGE	HYPERGEOM	HYPERGEOM	EDGE
	low volatility	HYPERGEOM	HYPERGEOM	EDGE	HYPERGEOM	HYPERGEOM	MLN
	low volatility and positive skewness	HYPERGEOM	HYPERGEOM	EDGE	HYPERGEOM	HYPERGEOM	EDGE
	high volatility and negative skewness	HYPERGEOM	HYPERGEOM	EDGE	HYPERGEOM	HYPERGEOM	MLN
	high volatility	HYPERGEOM	HYPERGEOM	EDGE	HYPERGEOM	HYPERGEOM	EDGE
	high volatility and positive skewness	HYPERGEOM	HYPERGEOM	MLN	EDGE	EDGE	MLN
3 months	low volatility and negative skewness	MLN	MLN	EDGE	MLN	MLN	MLN
	low volatility	HYPERGEOM	HYPERGEOM	SPLINE	HYPERGEOM	HYPERGEOM	EDGE
	low volatility and positive skewness	HYPERGEOM	HYPERGEOM	EDGE	HYPERGEOM	HYPERGEOM	EDGE
	high volatility and negative skewness	HYPERGEOM	HYPERGEOM	EDGE	HYPERGEOM	HYPERGEOM	HYPERGEOM
	high volatility	HYPERGEOM	HYPERGEOM	EDGE	HYPERGEOM	HYPERGEOM	EDGE
	high volatility and positive skewness	MLN	MLN	EDGE	HYPERGEOM	HYPERGEOM	MLN
6 months	low volatility and negative skewness	MLN	MLN	HYPERGEOM	MLN	MLN	EDGE
	low volatility	MLN	MLN	MLN	MLN	MLN	MLN
	low volatility and positive skewness	HYPERGEOM	HYPERGEOM	HYPERGEOM	HYPERGEOM	HYPERGEOM	SPLINE
	high volatility and negative skewness	MLN	MLN	HYPERGEOM	MLN	MLN	EDGE
	high volatility	MLN	MLN	HYPERGEOM	MLN	MLN	EDGE
	high volatility and positive skewness	MLN	MLN	EDGE	HYPERGEOM	HYPERGEOM	EDGE

Fig. 6. Best method according to RMISE criteria for high and low volatility dates

6.2.1 Best Performance of the DFCH and MLN model

The DFCH model was the best estimator of the "true" RND for almost all the dates tested with maturities of 1 and 3 months. The MLN method was the best estimator of the "true" 6-month RND. Overall, the DFCH method returns the best performance at capturing the true RND (the DFCH method has a lower RMISE 23 times and the MLN method 11 times). The EE and SML methods performed worse than all the other methods in terms of accuracy with the EE being the most biased model in the majority of scenarios (see figures B.9 and B.10).

6.2.2 Stability

In the stability analysis, the EE method outperforms all the other models. For the lower volatility dates, the EE method has the lower RIV for the majority of 1 and 3-month RNDs. The DFCH method has a lower RIV for most 6-month RNDs. For the high volatility dates the EE method has the best performance for the majority of scenarios.

7 Information contained in the option implied risk-neutral probability density function

Besides analyzing the accuracy and stability of the MLN, SML, DFCH and EE methods, we also estimated the end of month RNDs extracted from the USDBRL option prices for the period between June 2006 and February 2010 in order to compare the measures obtained for the three models tested and to interpret the information provided by these implied distributions.

7.1 Analyzing changes of implied pdf summary statistics over time

7.1.1 Comparing MLN, SML and DFCH

In this section we compare the summary statistics calculated for the MLN, SML, DFCH and EE methods and see if the results (regarding the uncertainty, the skewness and the probability of extreme moves) are similar for the methods considered, or if they show a similar trend.

The uncertainty around the mean, measured through the standard deviation of the estimated RNDs, has a strong correlation between the SML/DFCH, SML/EE and DFCH/EE pairs. The MLN/DFCH, MLN/SML and MLN/EE pairs have lower correlations for the standard deviation estimates. All methods capture the increase in volatility between September 2008 and February 2009 [7].

[7] This upward movement in volatility reached its maximum in November 2008 after a sequence of negative events (in September 2008 Government-sponsored enterprises Fannie Mae and Freddie Mac which owned or guaranteed about half (56.8%) of the U.S mortgage market were being placed into conservatorship of the FHFA (Federal Housing Finance Agency), Lehman Brothers filed for bankruptcy and the Bank of

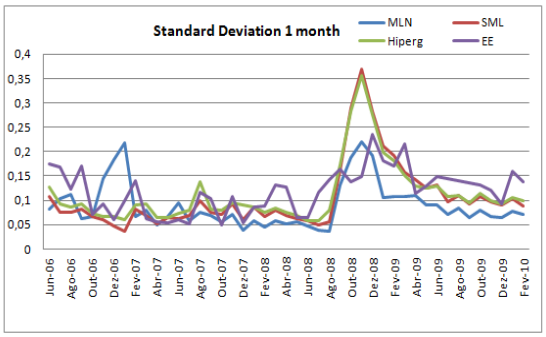

1 month			
ρ	SML	DFCH	EE
MLN	0,617	0,636	0,318
SML		0,990	0,588
DFCH			0,584

3 months			
ρ	SML	DFCH	EE
MLN	0,291	0,319	0,322
SML		0,978	0,866
DFCH			0,830

6 month			
ρ	SML	DFCH	EE
MLN	0,360	0,453	0,352
SML		0,985	0,883
DFCH			0,884

Fig. 7. Evolution of one month to maturity standard deviation and correlations between the standard deviations calculated through MLN, DFCH, SML and EE for the period between June 2006 and February 2010

Skewness is an indicator of the probability mass around the mean. If the implied distribution is positively skewed, the right tail is greater than the left tail and it suggests that market participants are positive about the future prices. However, a positively skewed distribution has an unweighted probability above the mean smaller than that below the mean (expected value is above the median and the mode), because the positive expectations lead to an upward revision of the expected price. Looking at figure 8, it is clear that for the period under consideration it is easier to find a trend for the implied skewness calculated for the DFCH and SML methods than for the MLN and EE methods (The MLN maintained a level close to 0.2 after December 2007 for "one month to maturity" term). The correlation level between the MLN method and the other methods is almost null or negative and the correlation between the SML/DFCH, SML/EE and DFCH/EE pairs is much lower when compared to the standard deviation estimations.

America purchased Merril Lynch, in October 2008 the US government bailed out Goldman Sachs and Morgan Stanley) that increased the risk aversion.

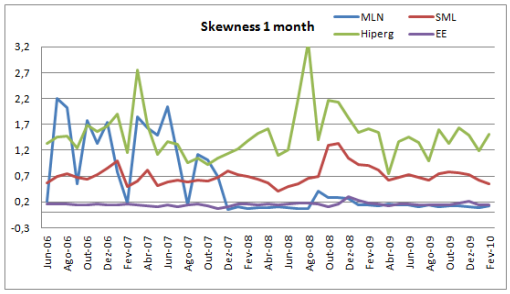

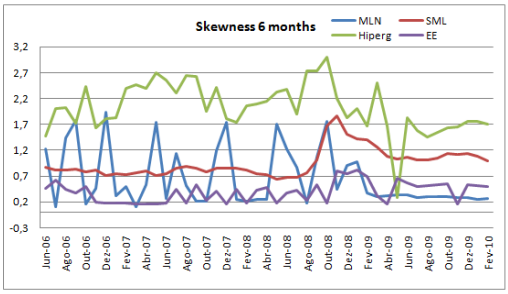

1 month			
ρ	SML	DFCH	EE
MLN	-0,046	0,079	-0,260
SML		0,378	0,223
DFCH			0,248

3 months			
ρ	SML	DFCH	EE
MLN	-0,262	0,014	-0,108
SML		0,543	0,215
DFCH			0,416

6 month			
ρ	SML	DFCH	EE
MLN	-0,061	0,190	-0,203
SML		-0,096	0,528
DFCH			-0,345

Fig. 8. Evolution of one month and six months to maturity skewness and correlations between the skewness calculated through MLN, DFCH, MLN and EE for the period between June 2006 and February 2010

As mentioned earlier in this work, the skewness is very sensitive to the tails of the distribution, which decreases the reliability of this measure. We therefore calculated the values for Pearson's skewness coefficients which are less sensitive to the tails of the distribution.

$$\text{Pearson median skewness} = \frac{E[X] - \text{median}}{\sigma} \tag{55}$$

$$\text{Pearson mode skewness} = \frac{E[X] - \text{mode}}{\sigma} \tag{56}$$

For both Pearson measures we saw lower correlation levels for higher maturities, which is shown in tables 6-3 and 6-4.

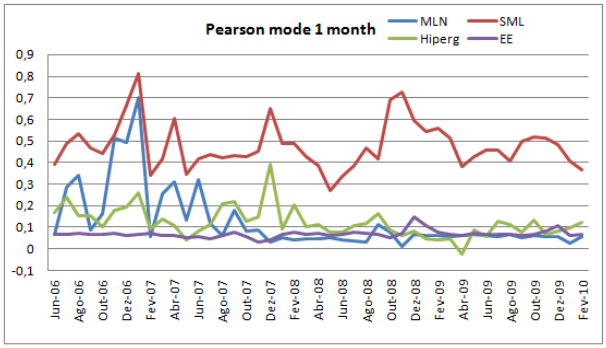

1 month			
ρ	SML	DFCH	EE
MLN	0,444	0,380	-0,089
SML		0,313	0,128
DFCH			-0,249

3 months			
ρ	SML	DFCH	EE
MLN	-0,057	0,364	-0,14909
SML		-0,225	0,155872
DFCH			0,069944

6 month			
ρ	SML	DFCH	EE
MLN	-0,034	0,403	-0,17549
SML		-0,025	0,366704
DFCH			-0,07733

Fig. 9. Evolution of one month to maturity Pearson mode and correlations between the Pearson mode calculated through MLN, DFCH, MLN and EE for the period between June 2006 and February 2010

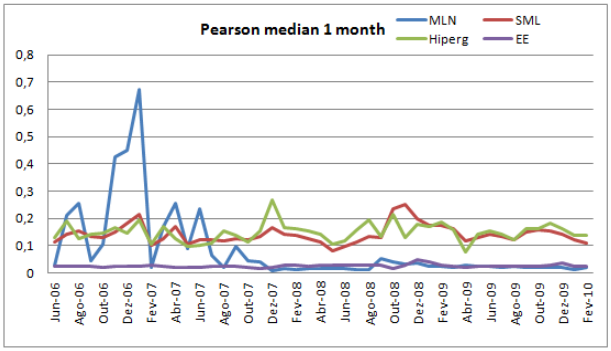

1 month			
ρ	SML	DFCH	EE
MLN	0,325	0,072	-0,143
SML		0,514	0,156
DFCH			0,151

3 months			
ρ	SML	DFCH	EE
MLN	-0,198	-0,327	-0,159
SML		0,569	0,149
DFCH			0,569

6 month			
ρ	SML	DFCH	EE
MLN	-0,103	0,025	-0,207
SML		0,386	0,442
DFCH			-0,022

Fig. 10. Evolution of one month to maturity Pearson median and correlations between the Pearson median calculated through MLN, DFCH, MLN and EE for the period between June 2006 and February 2010

As written earlier in this work, the kurtosis is highly sensitive to the tails of the distribution. As such, the reliability of the kurtosis measure is poor and should be interpreted with care. Like in the skewness analysis, the MLN method shows almost no changes after December 2007 and the estimations through the EE method have a low variability during this period. Once more, the correlation between the different methods was low.

In general terms, we observed that the RNDs corresponding to the real USDBRL quotes estimated through the EE and MLN methods did not capture the increase in skewness and kurtosis during the peak of the financial crisis (between September 2008 and February 2009), contrasting with the DFCH and SML models.

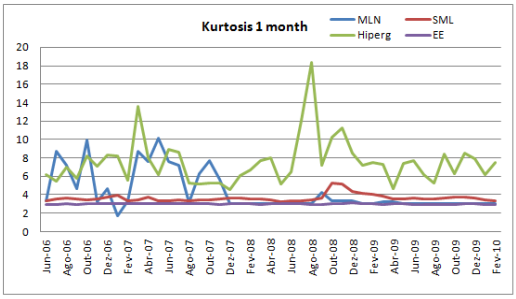

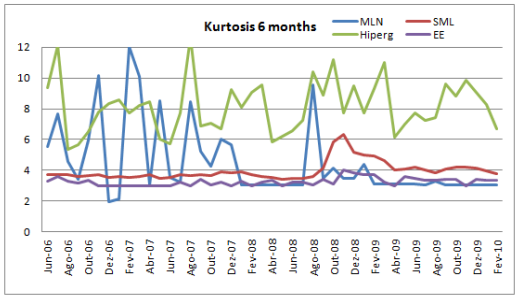

1 month			
ρ	SML	DFCH	EE
MLN	-0,212	0,010	0,009
SML		0,260	0,263
DFCH			-0,001

3 months			
ρ	SML	DFCH	EE
MLN	-0,227	0,163	0,152
SML		0,300	0,051
DFCH			0,389

6 month			
ρ	SML	DFCH	EE
MLN	-0,028	0,294	-0,174
SML		-0,229	0,661
DFCH			-0,371

Fig. 11. Evolution of 6 months to maturity Kurtosis and correlations between the kurtosis calculated through MLN, DFCH, MLN and EE for the period between June 2006 and February 2010

8 Conclusion

This work compared the DFCH method with the widely knowns SML, MLN and EE methods in the estimation of the Risk-Neutral Densities through option prices. The methodology adopted consisted of re-estimating the RNDs after adding a uniformly distributed random noise perturbation in theoretical option prices generated by Heston's stochastic volatility model for a set of different scenarios in order to test the ability of the different methods to recover the "true" RNDs under different market conditions. The "true" Heston model RNDs were produced using two approaches: in Chapter 5 we used the Heston parameters proposed in Cooper (1999) and in Chapter 6 we considered the Heston parameters that resulted from the calibration of this model for 6 low volatility dates (between October 2006 and March 2007) and 6 high volatility dates (between September 2008 and February 2009).

The four models tested were compared using two different approaches: analysis using the RMISE criteria which is a measure of the average distance between the "true" RND and the estimated ones and analysis using the summary statistics: mean, variance, skewness and kurtosis.

With the RMISE criteria we observed a higher performance of the DFCH method, especially for the low volatility dates (between October 2006 and March 2007) and high volatility dates (between September 2008 and February 2009). However, we noticed that the MLN method was slightly better than the DFCH model if we take into account only the Cooper scenarios and was superior in capturing the "true" 6-month RNDs of the USDBRL scenarios. In the stability analysis, we see the worst performance of the DFCH (higher RIV) in the Cooper scenarios, with the v weighting SML method showing the best results. Despite its lower stability, the DFCH method showed a higher overall quality as the "true" RND estimator in accordance with its estimated implied RNDs which recovered the true RNDs more closely in the majority of the cases. We also found that the v weighting scheme applied to the SML method only generates improvements in terms of stability, with the overall quality of the SML being unaffected. For the SML model we also tested a theoretically optimal λ (minimizes RMISE) and λ equal to 0.9 (because in the real world we do not know the optimal λ) as the smoothing parameter. We found that the comparative analysis of the methods tested was not sensitive to these two choices of the smoothing parameter.

The comparisons using the summary statistics were carried out in terms of accuracy (comparing the mean values of the summary statistics estimated from the Monte Carlo simulations and the "true" ones) and stability (standard deviation of the summary statistics). The results regarding the accuracy of skewness and kurtosis were better for the MLN and DFCH methods, with the EE method showing skewness and kurtosis values that are far from the "true" values in the majority of the cases. In terms of implied volatility, the SML method performed better in the majority of Cooper and USDBRL scenarios. In the stability analysis we conclude that the SML model significantly increases

its stability when the v weighting is adopted. The EE method was the most stable in the volatility estimation and the SML and EE models had the most stable estimations for skewness and kurtosis.

Despite also analyzing the summary statistics, we focused our analysis on the RMISE criteria because of the higher sensitivity of skewness and kurtosis to the tails of the distribution (RNDs can have an infinite variety of probability masses outside the range of available strike prices and those shapes are very dependent on the estimation methods used).

To sum up, we conclude that the DFCH method is the best estimator of the "true" RND in 1 and 3 months term and the MLN performs better in 6-months term according to the RMISE criterion. They outperform the SML and EE methods. It was also interesting to observe that the SML method did not outperform the MLN as an estimator of the "true" distribution according to the RMISE criterion (in Cooper (1999) the SML model was considered marginally better than the MLN model in terms of accuracy of summary statistics). In fact, despite being less stable than the SML method, the MLN method showed greater accuracy, having a lower RMISE than the SML model in most of the scenarios (Cooper, low volatility and high volatility dates). The SML was the most stable model, and its performance was enhanced when the v weighting was adopted. The EE method was not flexible enough to capture the higher moments of the true densities and obtained the more biased estimators.

In this work, we also obtained the USDBRL implied RNDs for the period between June 2006 and February 2010 in order to analyze the difference in the summary statistics estimated using DFCH, MLN, SML and EE methods. We observed a higher correlation between the models tested for the volatility and found a lower relation between the methods for the skewness, kurtosis, Pearson mode and Pearson median values, and more importantly, we saw that the DFCH and SML methods were more able to capture the increase in volatility, skewness and kurtosis during the peak of the financial crisis than the EE and SML models.

A Appendix 1

A.1 Mixture of hypergeometric functions

The function DFCH (density function based on confluent hypergeometric functions), that specifies European call pricing as a mixture of two confluent hypergeometric functions, is given by (see the details in Abadir and Rockinger (2003)):

$$C(X) = c_1 + c_2 X + l_{X>m_1} a_1((X-m_1)^{b_1})_1F_1(a_2; a_3; b_2(X-m_1)^{b_3}) \quad \text{(A.1)}$$
$$+ (a_4)_1F_1(a_5; a_6; b_4(X-m_2)^2),$$

where $a_{3,}a_6 \in \mathbb{N}$ and $b_2, b_4 \in \mathbb{R}^-$. The indicator function l represent a component of the density with bounded support.

The Kummer's function ${}_1F_1$ was defined in equation (19):

$$ {}_1F_1(\alpha,\beta,z) \equiv \sum_{j=0}^{\infty} \frac{(\alpha)_j}{\beta_j}\frac{z^j}{j!} \equiv 1 + \frac{\alpha}{\beta}z + \frac{\alpha(\alpha+1)}{\beta(\beta+1)}\frac{z^2}{2!} + \frac{\alpha(\alpha+1)(\alpha+2)}{\beta(\beta+1)(\beta+2)}\frac{z^3}{3!} + ... \tag{A.2} $$

The first derivative of ${}_1F_1(\alpha,\beta,z)$ is

$$ {}_1F_1(\alpha,\beta,z)' = \frac{\alpha}{\beta}[{}_1F_1(\alpha+1,\beta+1,z)]. \tag{A.3} $$

The Kummer's function has the following asymptotic representation for $X \in \mathbb{R}$ (see the details in Abadir (1999)),

$$ {}_1F_1(\alpha,\beta,z) = \begin{cases} \frac{\Gamma(\beta)}{\Gamma(\beta-a)}\left|z\right|^{-a}\left(1+O\left(\left(\frac{1}{2}\right)\right)\right), & \text{as } z \longrightarrow -\infty \\ \frac{\Gamma(\beta)}{\Gamma(a)}\left|z\right|^{a-c}\exp^{z}\left(1+O\left(\left(\frac{1}{2}\right)\right)\right), & \text{as } z \longrightarrow \infty \end{cases} \tag{A.4} $$

With the formula (A.3) we can obtain the implied probability density function which is given by the second derivative of $C(X)$ with respect to the strike price X.

$$ \begin{aligned} \frac{d^2C(X)}{dX^2} = e^{-r\tau}f(X) = l_{X>m1}a_1(X-m_1)^{b1-2}[b_1(b_1-1){}_1F_1(a_2;a_3;b_2(X-m_1)^{b_3}) \\ + \frac{a_2}{a_3}b_2b_3(2b_1+b_3-1)(X-m_1)^{b_3} \\ \times_1 F_1(a_2+1;a_3+1;b_2(X-m_1)^{b_3}) + \frac{a_2(a_2+1)}{a_3(a_3+1)}b_2^2b_3^2(X-m_1)^{2b_3} \\ \times_1 F_1(a_2+2;a_3+2;b_2(X-m_1)^{b_3})] \\ + 2a_4\frac{a_5}{a_6}b_4[{}_1F_1(a_5+1;a_6+1;b_4(X-m_2)^2) \\ + 2\frac{a_5+1}{a_6+1}b_4(X-m_2)^2{}_1F_1(a_5+2;a_6+2;b_4(X-m_2)^2)] \end{aligned} \tag{A.5} $$

The pdf (probability density function) derived from DFCH must be integrate to 1. To restrict the integral of $f(X)$ we derive

$$f(X) = \frac{dC(X)}{dX} = -\exp^{-r\tau}(1 - G(X)) = \tag{A.6}$$

$$= c_2 + l_{X>m_1} a_1 (X - m_1)^{b_1 - 1}[(b_1)_1 F_1(a_2; a_3; b_2(X - m_1)^{b_3}) \tag{A.7}$$

$$+ \frac{a_2}{a_3} b_2 b_3 ((X - m_1)^{b_3})_1 F_1(a_2 + 1; a_3 + 1; b_2(X - m_1)^{b_3})]$$

$$+ 2a_4 \frac{a_5}{a_6} b_4 (X - m_2)_1 F_1(a_5 + 1; a_6 + 1; b_4(X - m_2)^2)$$

In order to guarantee that $f(X)$ integrates to 1 between X_l and X_u we set,

$$\int_{X_l}^{X_u} f(X) dX = 1, \tag{A.8}$$

which is equivalent to

$$\frac{dC(X_l)}{dX} = G(X_l) - 1 = -1, \tag{A.9}$$

$$\frac{dC(X_u)}{dX} = G(X_u) - 1 = 0. \tag{A.10}$$

Solving the restrictions on equations (A.9) and (A.10), we obtain explicit formulas for the parameters c_2 and a_4. If we assume that $X_l < m_1$, from the constrain set in equation (A.9), we conclude that c_2 is defined as

$$c_2 = -1 - 2a_4 \frac{a_5}{a_6} b_4 (X_l - m_2)_1 F_1(a_5 + 1, a_6 + 1, b_4(X_l - m_2)^2) \tag{A.11}$$

Applying the restriction on X_u defined in equation (A.10), we get c_2 plus the other terms of (A.6) which give the following explicit formula for c_2

$$c_2 = -a_1 (X_u - m_1)^{b_1 - 1}[(b_1)_1 F_1(a_2; a_3; b_2(X_u - m_1)^{b_3}) \tag{A.12}$$

$$+ \frac{a_2}{a_3} b_2 b_3 ((X_u - m_1)^{b_3})_1 F_1(a_2 + 1; a_3 + 1; b_2(X_u - m_1)^{b_3})]$$

$$- 2a_4 \frac{a_5}{a_6} b_4 (X_u - m_2)_1 F_1(a_5 + 1; a_6 + 1; b_4(X_u - m_2)^2).$$

If we compare equations (A.11) and (A.12), we get an explicit formula for a_4,

$$a_4 = \left\{ \begin{array}{c} 1 - a_1 (X_u - m_1)^{b_1 - 1}[(b_1)_1 F_1(a_2; a_3; b_2(X_u - m_1)^{b_3}) \\ + \frac{a_2}{a_3} b_2 b_3 ((X_u - m_1)^{b_3})_1 F_1(a_2 + 1; a_3 + 1; b_2(X_u - m_1)^{b_3})] \end{array} \right\} \tag{A.13}$$

$$\div \left\{ \begin{array}{c} 2\frac{a_5}{a_6} b_4 [(X_u - m_2)_1 F_1(a_5 + 1; a_6 + 1; b_4(X_u - m_2)^2) \\ -(X_l - m_2)_1 F_1(a_5 + 1, a_6 + 1, b_4(X_l - m_2)^2)] \end{array} \right\}$$

In Abadir and Rockinger (2003), the assumptions $b_1 = 1 + a_2 b_3$; $a_5 = -\frac{1}{2}$ and $a_6 = \frac{1}{2}$ were applied in equations (A.11) and (A.13). Using the asymptotic representation of Kummer's function in equation (A.4), equation (A.11) simplifies to

$$c_2 = -1 + a_4\sqrt{-b_4 \times \pi} \tag{A.14}$$

and equation (A.13) simplifies to

$$a_4 = \frac{1}{2\sqrt{-b_4\pi}}\left[1 - a_1(-b_2)^{-a_2}\frac{\Gamma(a_3)}{\Gamma(a_3 - a_2)}\right]. \tag{A.15}$$

This formula was deduced by simplifying the two terms of equation (A.13) separately. The first term is

$$\begin{aligned} &1 - a_1(X_u - m_1)^{b_1-1}[(b_1){}_1F_1(a_2; a_3; b_2(X_u - m_1)^{b_3}) \\ &+ \frac{a_2}{a_3}b_2 b_3((X_u - m_1)^{b_3}){}_1F_1(a_2 + 1; a_3 + 1; b_2(X_u - m_1)^{b_3})] \end{aligned} \tag{A.16}$$

applying the relation ${}_1F_1(\alpha, \beta, z) = \exp^z {}_1F_1(\beta - \alpha, \beta, -z)$ [8] we continue the simplification of the first term

$$\begin{aligned} &= 1 - a_1(X_u - m_1)^{b_1-1} b_1 \frac{\Gamma(a_3)}{\Gamma(a_3 - a_2)}(-b_2(X_u - m_1)^{b_3})^{-a_2} \\ &- a_1(X_u - m_1)^{b_1-1}\frac{a_2}{a_3}b_2 b_3 (X_u - m_1)^{b_3}\frac{\Gamma(a_3 + 1)}{\Gamma(a_3 - a_2)}(-b_2(X_u - m_1)^{b_3})^{-a_2-1}. \end{aligned} \tag{A.17}$$

Taking into account that $\Gamma(a_3 + 1) = a_3!$ we transform the $\Gamma(a_3 + 1)$ into $\Gamma(a_3) \times a_3$, which gives

$$\begin{aligned} &1 - a_1(X_u - m_1)^{b_1 - a_2 b_3 - 1} b_1 \frac{\Gamma(a_3)}{\Gamma(a_3 - a_2)}(-b_2)^{-a_2} \\ &- a_1(X_u - m_1)^{b_1 - a_2 b_3 - 1} a_2 b_3 \frac{\Gamma(a_3)}{\Gamma(a_3 - a_2)}(-b_2)^{-a_2} b_2 (-b_2)^{-1} \\ &= 1 - a_1(-b_2)^{-a_2}\frac{\Gamma(a_3)}{\Gamma(a_3 - a_2)}. \end{aligned} \tag{A.18}$$

Applying the same transformation set in the first term ${}_1F_1(\alpha, \beta, z) = e^z {}_1F_1(\beta - \alpha, \beta, -z)$, the second term of equation (A.13) is

$$-4(-b_4)^{\frac{1}{2}}\frac{\Gamma(a_6 + 1)}{\Gamma(a_6 - a_5)} = -4\sqrt{-b_4}\frac{\Gamma(\frac{3}{2})}{\Gamma(1)} = 2\sqrt{b_4(\Gamma(\frac{3}{2})^2)2^2} = 2\sqrt{b_4\pi} \tag{A.19}$$

[8] This transformation is shown by Karim Abadir (1999) in "An introduction to hypergeometric functions for economiste"

Taking into account that $(\Gamma(\frac{3}{2})^2)2^2 = \pi$, we have that

$$4\sqrt{-b_4}\Gamma(\frac{3}{2}) = 2\sqrt{-b_4(\Gamma(\frac{3}{2})^2)2^2} = 2\sqrt{-b_4\pi}. \tag{A.20}$$

A.2 Edgeworth Expansion

After imposing $k_1(F) = k_1(L)$ and $k_2(F) = k_2(L)$ the option price formula becames:

$$C(F) = e^{-rt}\int_{-\infty}^{\infty} \max(0, S_t - X) f(S_T) dS = C(A) \tag{A.21}$$

$$-e^{-rt}\frac{k_3(F) - k_3(L)}{3!}\int_{-\infty}^{\infty} \max(0, S_t - X)\frac{d^3 l(S_T)}{dS_T^3} dS \tag{A.22}$$

$$+e^{-rt}\frac{(k_4(F) - k_4(L)) + 3(k_2(F) - k_2(L))^2}{4!}\int_{-\infty}^{\infty} \max(0, S_t - X)\frac{d^4 l(S_T)}{dS_T^4} dS + \varepsilon$$

Integrating by parts we know that $\int_X^\infty (S_t - X)\frac{d^j a(S_T)}{dS_T^j} dS_t = \left[(S_t - X)\frac{d^{j-1} a(S_T)}{dS_T^{j-1}}\right]_X^\infty - \int_X^\infty (S_t - X) dS_t = \frac{d^{j-2} a(K)}{dS_T^{j-2}}$, which gives the following call option formula written in terms of cumulants:

$$C(F) = C(A) - e^{-rt}\frac{k_3(F) - k_3(L)}{3!}\frac{dl(S_T)}{dS_T} \tag{A.23}$$

$$+e^{-rt}\frac{(k_4(F) - k_4(L)) + 3(k_2(F) - k_2(L))^2}{4!}\frac{dl^2(S_T)}{dS_T^2} dS + \varepsilon$$

B Appendix 2

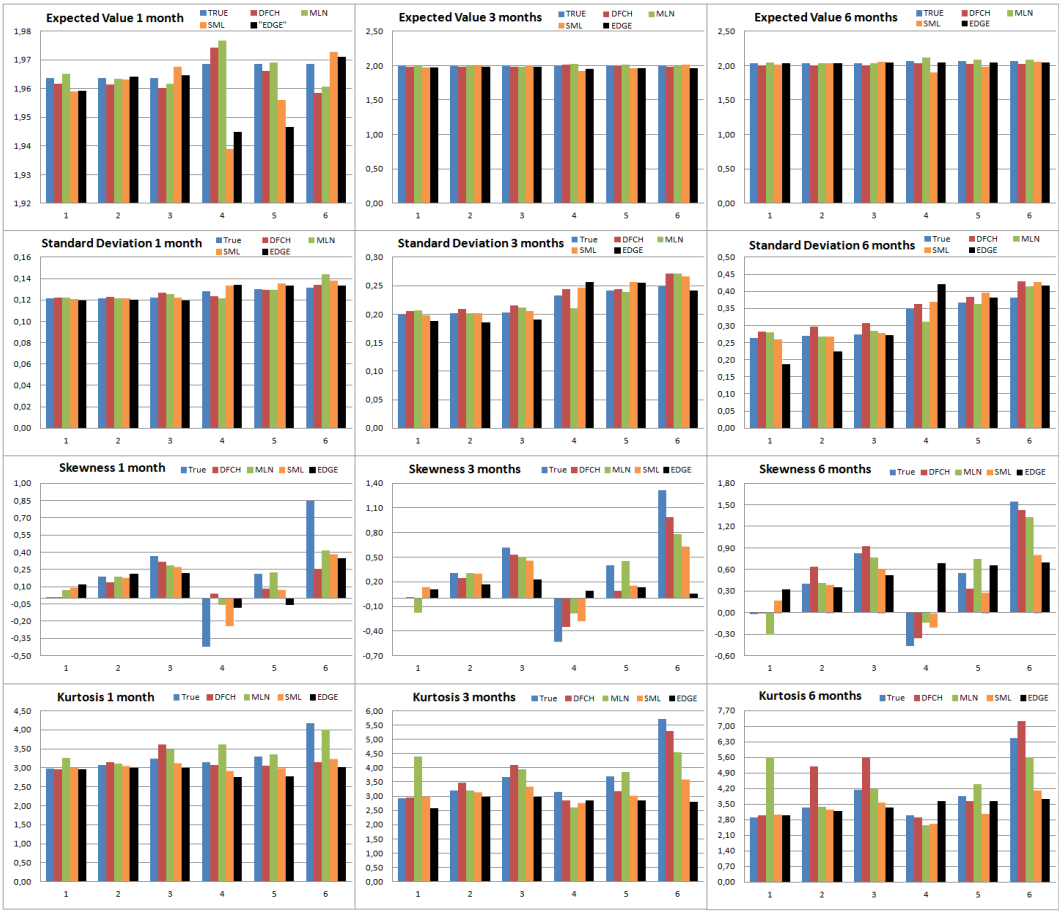

Fig. B.1. Cooper scenarios: Summary statistics obtained for Heston model (true density) and mean of summary statistics obtained for DFCH, MLN, SML and EE methods. The results estimated for the SML method were processed with v weighting and with the smoothing that minimizes RMISE.

Fig. B.2. Cooper Scenarios: Standard Deviation of the summary statistics for the SML, MLN, DFCH and EE methods

		With v weighting						Without v weighting					
		SML (λ=0,9)			SML (λ that minimizes RMISE)			SML (smooth=0,9)			SML (min RMISE)		
	Scenario	1 month	3 months	6 months	1 month	3 months	6 months	1 month	3 months	6 months	1 month	3 months	6 months
Variance	1	0,0002	0,0004	0,0005	0,0002	0,0004	0,0005	0,0004	0,0008	0,0054	0,0003	0,0007	0,0048
	2	0,0002	0,0004	0,0005	0,0002	0,0004	0,0005	0,0003	0,0006	0,0011	0,0003	0,0006	0,0010
	3	0,0002	0,0004	0,0006	0,0002	0,0004	0,0006	0,0003	0,0006	0,0010	0,0003	0,0006	0,0009
	4	0,0002	0,0004	0,0006	0,0002	0,0004	0,0006	0,0004	0,0010	0,0015	0,0004	0,0008	0,0013
	5	0,0002	0,0005	0,0008	0,0002	0,0005	0,0008	0,0003	0,0006	0,0009	0,0003	0,0006	0,0008
	6	0,0003	0,0006	0,0009	0,0003	0,0005	0,0009	0,0003	0,0006	0,0010	0,0003	0,0006	0,0010
Skewness	1	0,0029	0,0015	0,0009	0,0031	0,0015	0,0008	0,0193	0,0212	0,1623	0,0193	0,0214	0,1588
	2	0,0029	0,0022	0,0016	0,0030	0,0022	0,0016	0,0141	0,0104	0,0113	0,0136	0,0102	0,0110
	3	0,0030	0,0020	0,0015	0,0030	0,0020	0,0014	0,0109	0,0064	0,0053	0,0112	0,0065	0,0050
	4	0,0035	0,0024	0,0024	0,0035	0,0026	0,0023	0,0343	0,0253	0,0152	0,0348	0,0245	0,0148
	5	0,0049	0,0034	0,0026	0,0050	0,0033	0,0026	0,0109	0,0054	0,0033	0,0112	0,0053	0,0032
	6	0,0033	0,0020	0,0017	0,0032	0,0023	0,0017	0,0060	0,0026	0,0020	0,0060	0,0026	0,0020
Kurtosis	1	0,0004	0,0005	0,0002	0,0004	0,0005	0,0003	0,0092	0,0116	0,0696	0,0065	0,0092	0,0561
	2	0,0006	0,0017	0,0014	0,0006	0,0016	0,0014	0,0083	0,0088	0,0125	0,0073	0,0088	0,0104
	3	0,0021	0,0024	0,0017	0,0021	0,0023	0,0015	0,0102	0,0075	0,0095	0,0087	0,0065	0,0079
	4	0,0027	0,0019	0,0006	0,0028	0,0020	0,0006	0,0038	0,0027	0,0054	0,0064	0,0038	0,0047
	5	0,0009	0,0023	0,0025	0,0009	0,0022	0,0025	0,0055	0,0042	0,0037	0,0049	0,0038	0,0035
	6	0,0037	0,0030	0,0039	0,0036	0,0029	0,0037	0,0077	0,0041	0,0045	0,0070	0,0039	0,0044

Fig. B.3. Cooper Scenarios: Standard deviation of the summary statistics for the SML method under 4 scenes: with or without v weighting and for each weighting approach using a smoothing parameter that minimizes RMISE or a smoothing parameter with a value of 0,9.

Fig. B.4. Cooper Scenarios: Values for RMISE, RISB and RIV. The results shown for the SML method were processed with v weighting and the parameter that minimizes RMISE

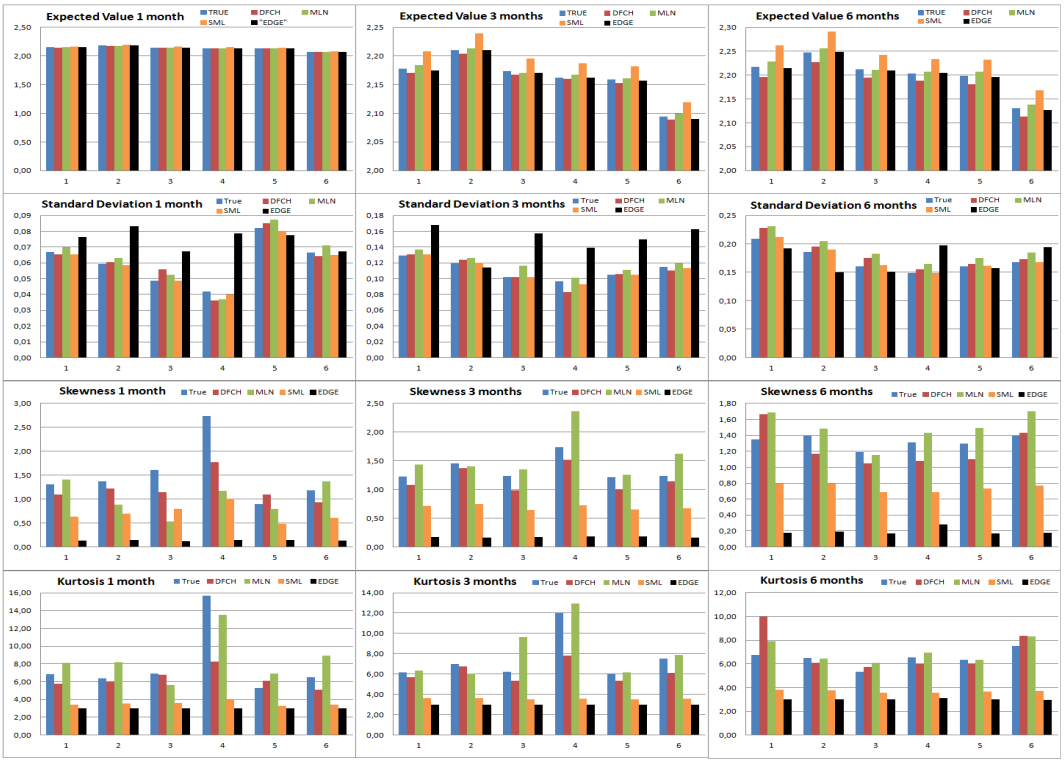

Fig. B.5. USDBRL scenarios - Low Volatility Dates: Summary statistics obtained for Heston model (true density) and mean of summary statistics obtained for DFCH, MLN, SML and EE methods.

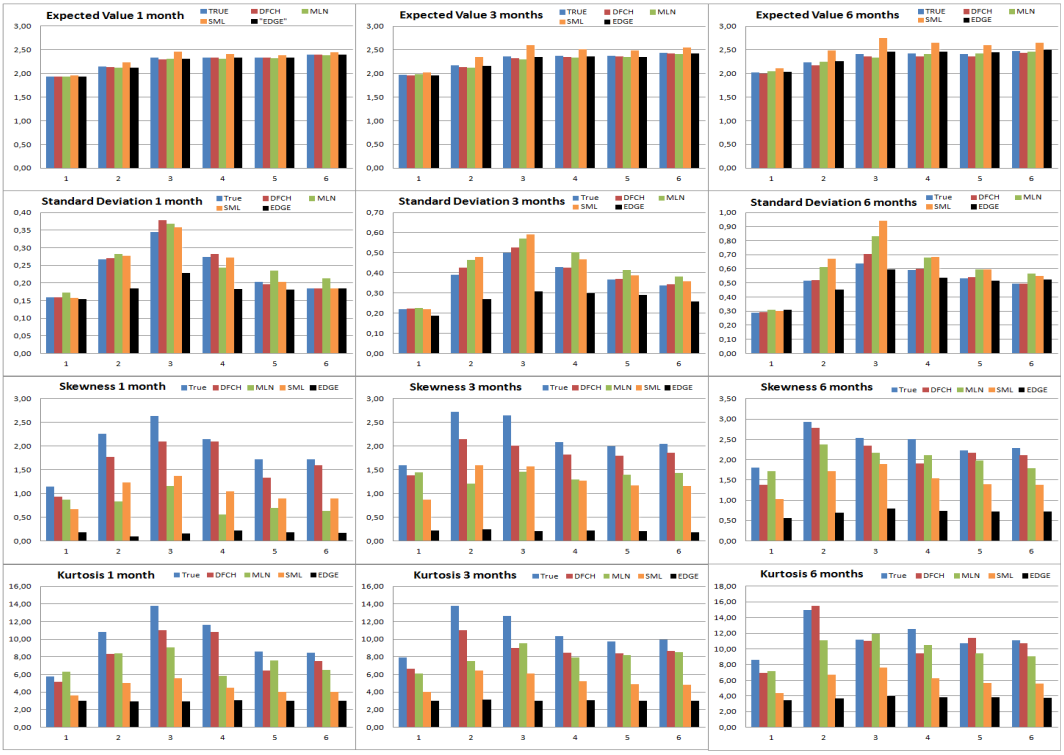

Fig. B.6. USDBRL scenarios - High Volatility Dates: Summary statistics obtained for Heston model (true density) and mean of summary statistics obtained for DFCH, MLN, SML and EE methods.

Fig. B.7. USDBRL scenarios - Low Volatility Dates: Standard Deviation of the summary statistics for the SML, MLN and DFCH methods

Fig. B.8. USDBRL scenarios - High Volatility Dates: Standard Deviation of the summary statistics for the SML, MLN and DFCH methods

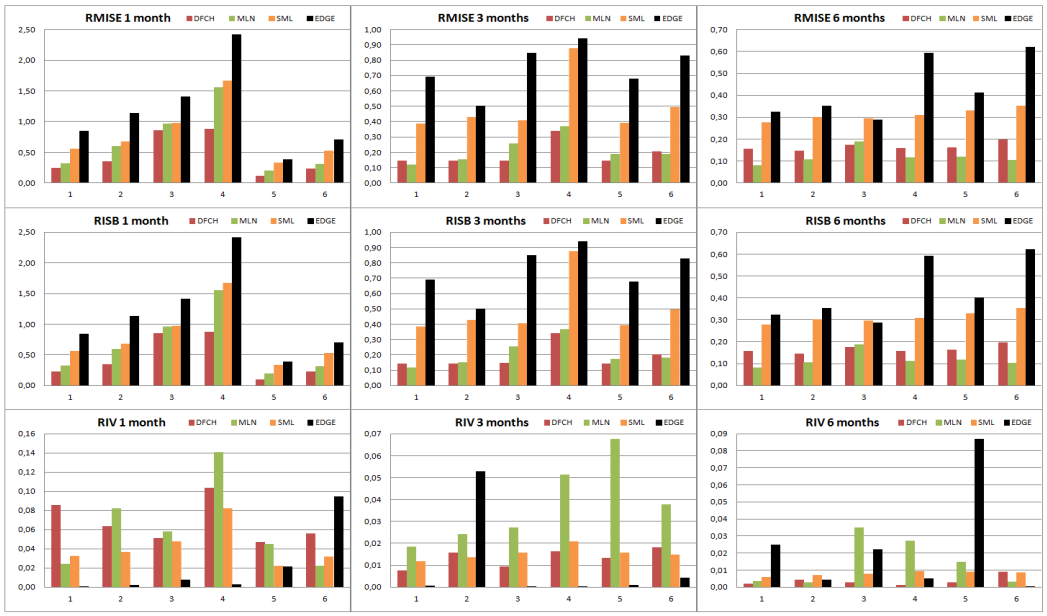

Fig. B.9. USDBRL scenarios - Low Volatility Dates: Values for RMISE, RISB and RIV.

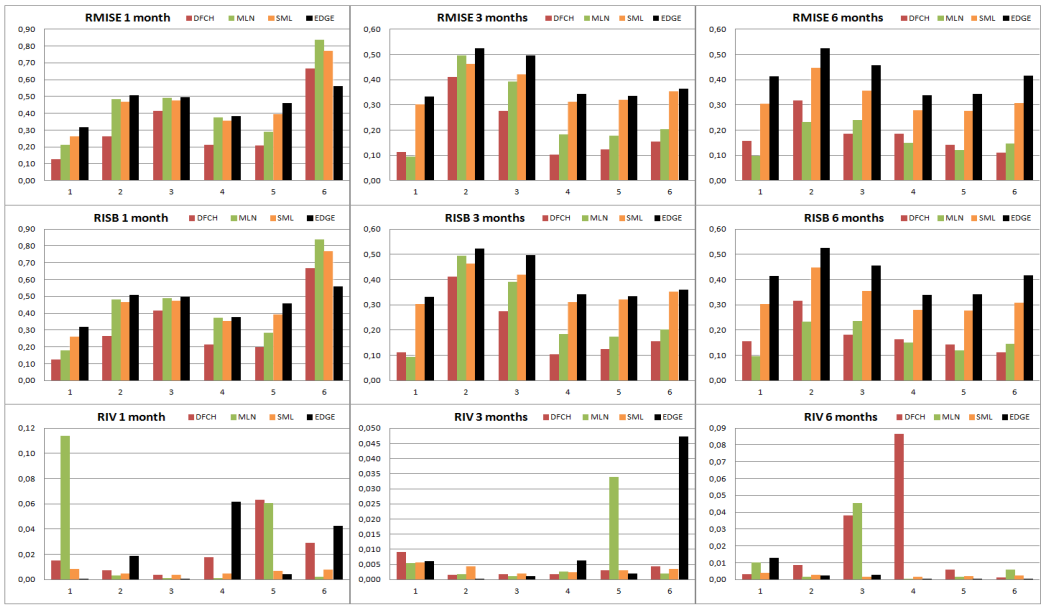

Fig. B.10. USDBRL scenarios - High Volatility Dates: Values for RMISE, RISB and RIV.

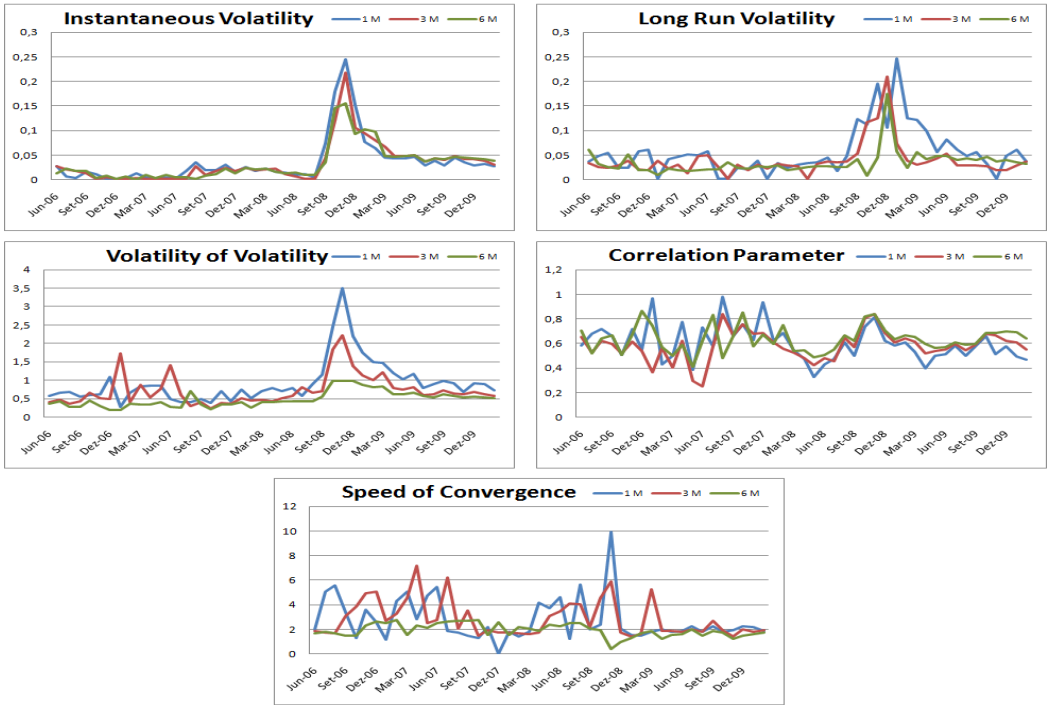

Fig. B.11. Heston model parameters obtained through calibration between June 2006 and February 2010

References

Abadir, K. M. (1999). *An introduction to hypergeometric functions for economists*. Econometric Reviews 18 (2003).

Abadir, K. M. and Rockinger, M (2003). *Density functionals, with an option-pricing application*. Econometric Theory 19, 778–811.

Santos, A. D. (2011). Implied probability density functions: Estimation using hypergeometric, spline and lognormal functions. Master Thesis, ISEG-UTL.

Arrow, K. J. and Debreu, G. (1954). *Existence of an equilibrium for a competitive economy*. Econometrica 22:265-290.

Arrow, K. J. (1964). *The Role of Securities in the Optimal Allocation of Risk-Bearing*.Review of Economic Studies, 31, No. 2 (April), pages 91-96.

Bahra, B. (1997). *Implied risk-neutral probability density functions from option prices: Theory and application*. Working Paper, Bank of England.

Black, F. and Sholes, M. (1973), *Pricing of Options and Corporate Liabilities*, Journal of Political Economy, 81, pages 637-659.

Bliss, R. and Panigirtzoglou, N. (2002). *Testing the stability of implied probability density functions*. Journal of Banking and Finance 26, 381–422.

Breeden, D. T. and Litzenberger, R. H. (1978). *Prices of state-contingent claims implicit in option prices*. Journal of Business 51, 621–51.

Bu, R. and Hadri, K. (2007). *Estimating option implied risk-neutral densities using spline and hypergeometric functions*. Journal of Econometrics 10, 216-244.

Campa, J.C., Chang, P.H.K., and Reider, R.L. (1997). *ERM bandwidths for EMU and after: evidence from foreign exchange options*. Economic Policy, 55–87.

Cooper, N. (1999).*Testing techniques for estimating implied RNDs from the prices of European and American options*. Working Paper, Bank of England.

Cox, J. and Ross, S. (1976), *The Valuation of Options for Alternative Stochastic Processes*, Journal of Financial Economics, 3, pages 145-66.

Corrado, C.J., Su, T., 1996. S&P500 index option tests of Jarrow and Rudd's approximate option valuation formula. Journal of Futures Markets 6, 611–629.

Espen, G. H. (2007). *Option Pricing Formulas, second edition.*

Heston, S. (1993). *A Closed-Form Solution for Options with Stochastic Volatility With Applications to Bond and Currency Options*, The Review of Financial Studies, Vol 6, No 2, pp 327-343.

Jarrow, R. and Rudd, A. (1982), Approximate option valuation for arbitrary stochastic processes. Journal of Financial Economics, 10, 347-369.

Jondeau, E. and Rockinger, M. (2000). *Reading the smile: The message conveyed by methods which infer risk neutral densities*. Journal of International Money and Finance 19, 885–915.

Jondeau, E., Poon, S.H and Rockinger, M. (2006). *Financial Modeling Under Non-Gaussian Distributions.*

Kendall, M (1945), The Advanced Theory of Statistics, Vol 1, 2th ed.

Lee, S. H. (2008). *Three essays on estimation of risk neutral measures using option pricing models*. Dissertation presented for the Degree Doctor of Philosophy in the Graduate School of The Ohio State University

Malz, A.M., (1996). Options-based estimates of the probability distribution of exchange rates and currency excess returns, mimeo. Federal Reserve Bank of New York.

Malz, A. M. (1997). *Estimating the probability distribution of the future exchange rate from options prices*. Journal of Derivatives, Winter, pages 18-36.

Melick, W. R. and Thomas, C. P. (1997). *Recovering an Asset's Implied PDF from Option Prices: An Application to Crude Oil during the Gulf Crisis*, Journal of Financial and Quantitative Analysis, Vol 32, pages 91-115.

Shimko, D. C. (1993), *Bounds of probability*, Risk 6, pages 33-37.